sites at the termini was inserted into the XhoI/NheI site of the targeted insertion construct for AP2-O::GFP, in frame with the GFP gene. Plasmids containing these constructs were separated from plasmid backbone by digestion with XhoI and NotI and then used for transfection. The PCR primer pairs used for preparing the targeted insertion constructs and Southern hybridization probe are listed in Table S5.

DNA microarray analysis

Ookinetes were cultured for 12 h. Five biologically independent samples were prepared from AP2-O::Sp and *AP2-O* (–) parasites. *AP2-O* (–) parasites were used as controls. Extraction of total RNA and the following microarray analyses were performed using the same procedure as described in Yuda *et al.*, (2009). Genes that increased more than threefold compared with *AP2-O* (–) parasites, for at least two probes, were selected as being induced in AP2-O::Sp parasites. From the selected genes, those having no orthologues in *P. falciparum* were excluded, because such genes are usually located in the subtelomeric regions and belong to multigene families such as the bir gene family. Microarray data have been submitted to Gene Expression Omnibus (GEO) under Accession No. GSE18910.

ChIP-quantitative PCR assays

ChIP was performed using essentially the same procedure as described previously (Yuda *et al.*, 2009). DNA fragments obtained by IP were analysed by real-time PCR using an iCycler iQ Real-Time Detection System (Bio-Rad, Hercules, CA, USA) with the primers listed in Table S7.

Acknowledgements

This work was supported by the Ministry of Education, Science, Culture, and Sports of Japan (Grant 20249023, 21022019 and 21659105 to M.Y., Grant 21022032 and 21790406 to S.I. and Grant 21790403 to I.K.) and by the Ministry of Health, Labor, and Welfare (Research Grant for Research on Emerging and Re-emerging Infectious Diseases to H.K.).

References

Aly, A.S., and Matuschewski, K. (2005) A malarial cysteine protease is necessary for Plasmodium sporozoite egress from oocysts. *J Exp Med* **202:** 225–230.

Amino, R., Giovannini, D., Thiberge, S., Gueirard, P., Boisson, B., Dubremetz, J.F., *et al.* (2008) Host cell traversal is important for progression of the malaria parasite through the dermis to the liver. *Cell Host Microbe* **3:** 88–96.

Balaji, S., Babu, M.M., Iyer, L.M., and Aravind, L. (2005) Discovery of the principal specific transcription factors of Apicomplexa and their implication for the evolution of the AP2-integrase DNA binding domains. *Nucleic Acids Res* **33:** 3994–4006.

De Silva, E.K., Gehrke, A.R., Olszewski, K., Leon, I., Chahal, J.S., Bulyk, M.L., and Llinas, M. (2008) Specific DNA-binding by apicomplexan AP2 transcription factors. *Proc Natl Acad Sci USA* **105:** 8393–8398.

Dessens, J.T., Siden-Kiamos, I., Mendoza, J., Mahairaki, V., Khater, E., Vlachou, D., *et al.* (2003) SOAP, a novel malaria ookinete protein involved in mosquito midgut invasion and oocyst development. *Mol Microbiol* **49:** 319–329.

Ishino, T., Yano, K., Chinzei, Y., and Yuda, M. (2004) Cell-passage activity is required for the malarial parasite to cross the liver sinusoidal cell layer. *PLoS Biol* **2:** E4.

Ishino, T., Chinzei, Y., and Yuda, M. (2005) A Plasmodium sporozoite protein with a membrane attack complex domain is required for breaching the liver sinusoidal cell layer prior to hepatocyte infection. *Cell Microbiol* **7:** 199–208.

Jofuku, K.D., den Boer, B.G., Van Montagu, M., and Okamuro, J.K. (1994) Control of Arabidopsis flower and seed development by the homeotic gene APETALA2. *Plant Cell* **6:** 1211–1225.

Kariu, T., Yuda, M., Yano, K., and Chinzei, Y. (2002) MAEBL is essential for malarial sporozoite infection of the mosquito salivary gland. *J Exp Med* **195:** 1317–1323.

Matuschewski, K., Ross, J., Brown, S.M., Kaiser, K., Nussenzweig, V., and Kappe, S.H. (2002) Infectivity-associated changes in the transcriptional repertoire of the malaria parasite sporozoite stage. *J Biol Chem* **277:** 41948–41953.

Menard, R., Sultan, A.A., Cortes, C., Altszuler, R., van Dijk, M.R., Janse, C.J., *et al.* (1997) Circumsporozoite protein is required for development of malaria sporozoites in mosquitoes. *Nature* **385:** 336–340.

Moreira, C.K., Templeton, T.J., Lavazec, C., Hayward, R.E., Hobbs, C.V., Kroeze, H., *et al.* (2008) The Plasmodium TRAP/MIC2 family member, TRAP-like protein (TLP), is involved in tissue traversal by sporozoites. *Cell Microbiol* **10:** 1505–1516.

Mueller, A.K., Labaied, M., Kappe, S.H., and Matuschewski, K. (2005) Genetically modified Plasmodium parasites as a protective experimental malaria vaccine. *Nature* **433:** 164–167.

Young, J.A., Johnson, J.R., Benner, C., Yan, S.F., Chen, K., Le Roch, K.G., *et al.* (2008) In silico discovery of transcription regulatory elements in *Plasmodium falciparum*. *BMC Genomics* **9:** 70.

Yuda, M., Iwanaga, S., Shigenobu, S., Mair, G.R., Janse, C.J., Waters, A.P., *et al.* (2009) Identification of a transcription factor in the mosquito-invasive stage of malaria parasites. *Mol Microbiol* **71:** 1402–1414.

Supporting information

Additional supporting information may be found in the online version of this article.

Please note: Wiley-Blackwell are not responsible for the content or functionality of any supporting materials supplied by the authors. Any queries (other than missing material) should be directed to the corresponding author for the article.

nature medicine

Human P-selectin glycoprotein ligand-1 is a functional receptor for enterovirus 71

Yorihiro Nishimura[1], Masayuki Shimojima[2], Yoshio Tano[1,3], Tatsuo Miyamura[1], Takaji Wakita[1] & Hiroyuki Shimizu[1]

Enterovirus 71 (EV71) is a major causative agent of hand, foot and mouth disease (HFMD), a common febrile disease occurring mainly in young children. Although clinical manifestations of HFMD are usually mild and self limiting, a severe EV71 outbreak can lead to a diverse array of neurological diseases. Identification of the specific cellular receptors is crucial for elucidating the mechanism of early virus-host interactions and the pathogenesis of enteroviruses[1]. Here we identify human P-selectin glycoprotein ligand-1 (PSGL-1; CD162), a sialomucin membrane protein expressed on leukocytes that has a major role in early stages of inflammation[2–4], as a functional receptor for EV71 using an expression cloning method by panning[5]. The N-terminal region of PSGL-1 binds specifically to EV71. Stable PSGL-1 expression allowed EV71 entry and replication, and development of cytopathic effects in nonsusceptible mouse L929 cells. Five out of eight EV71 strains bound soluble PSGL-1 and used intact PSGL-1 as the primary receptor for infection of Jurkat T cells. Three other EV71 strains did not use PSGL-1, suggesting the presence of strain-specific replication of EV71 in leukocytes. EV71 replicated in nonleukocyte cell lines in a PSGL-1–independent manner, indicating the presence of alternative receptor(s) for EV71. The identification of PSGL-1 as a receptor for EV71 sheds new light on a role for PSGL-1–positive leukocytes in cell tropism and pathogenesis during the course of HFMD and other EV71-mediated diseases.

EV71 and coxsackievirus A16 (CVA16) belong to the human enterovirus species A of the genus *Enterovirus*[6] and are the major causative agents of HFMD. EV71 may cause various neurological diseases, such as aseptic meningitis, acute flaccid paralysis and fatal neurogenic pulmonary edema. Severe EV71 outbreaks have been reported periodically throughout the world, representing a major public health concern, particularly in the Asia-Pacific region[7–9]. During large outbreaks of EV71, individuals with severe EV71-associated encephalitis and neurogenic pulmonary edema showed a marked depletion of T cells and high levels of proinflammatory cytokines[10,11]. Because of this T cell involvement, we generated a retroviral complementary DNA (cDNA) library from Jurkat T cells that are susceptible to EV71 infection[12] and used it for expression cloning[5] to identify a receptor that specifically binds EV71 virions (EV71-1095 strain, **Supplementary Table 1**). Transduction of mouse myeloma P3X63Ag8U.1 (P3U1) cells with the Jurkat cDNA library resulted in the formation of four colonies that bound EV71-1095–coated dishes, all of which encoded human PSGL-1 (*SELPLG*) (**Fig. 1a** and **Supplementary Fig. 1**).

To confirm the specific binding of PSGL-1 to EV71-1095, we used 293T cells, which express undetectable amounts of endogenous PSGL-1. Transient expression of human PSGL-1 on 293T cells markedly increased the binding of EV71-1095 to 293T cells (**Fig. 1b**); however, expression of control ligands (sialomucin proteins CD34 and CD43) and mouse Psgl-1 did not (**Supplementary Fig. 2**). To identify the region of human PSGL-1 that is important for EV71 binding, we first constructed a chimeric PSGL-1 (hmPSGL-1) containing amino acids 1–61 of the human PSGL-1 followed by amino acids 63–397 of mouse Psgl-1 (**Supplementary Fig. 3a,b**). EV71-1095 bound hmPSGL-1 expressed on 293T cells (**Supplementary Fig. 3c**). To confirm this finding, we examined whether monoclonal antibodies (mAbs) recognizing PSGL-1 (KPL1 (refs. 13,14) and PL2 (ref. 15); **Fig. 1a**) block the PSGL-1–EV71 interaction. KPL1, which blocks P-selectin binding to PSGL-1 (ref. 13), inhibited EV71-1095 binding to 293T cells transiently expressing PSGL-1 in a dose-dependent manner; however, PL2, which does not block binding to P-selectin, did not (**Fig. 1c**). These findings suggest that the N-terminal region (amino acids 42–61) of human PSGL-1 is crucial for interactions with EV71-1095.

To test whether PSGL-1 is involved in the later steps of viral entry after binding to cells, we used mouse cells that do not support EV71 infection. Mouse myeloma P3U1 cells expressing human PSGL-1 did not support efficient EV71 replication (data not shown). Therefore, we obtained an L929 cell clone (L-PSGL-1.1) that stably expresses high amounts of human PSGL-1 (**Fig. 2a**). L-PSGL-1.1 cells showed a cytopathic effect 4 d after infection, and we detected EV71 antigen by immunofluorescence in the infected L-PSGL-1.1 cells (**Fig. 2b**). The development of cytopathic effect and detection of viral antigens induced by EV71-1095 infection was markedly inhibited by KPL1 (**Fig. 2b**), but not by PL2 (data not shown), as were the replication kinetics of EV71-1095 in infected L-PSGL-1.1 cells (**Fig. 2c,d**),

[1]Department of Virology II, National Institute of Infectious Diseases, Musashimurayama-shi, Tokyo, Japan. [2]Division of Virology, Department of Microbiology and Immunology, Institute of Medical Science, University of Tokyo, Minato-ku, Tokyo, Japan. [3]Present address: Japan Poliomyelitis Research Institute, Higashimurayama-shi, Tokyo, Japan. Correspondence should be addressed to H.S. (hshimizu@nih.go.jp).

Received 2 December 2008; accepted 6 April 2009; published online 21 June 2009; doi:10.1038/nm.1961

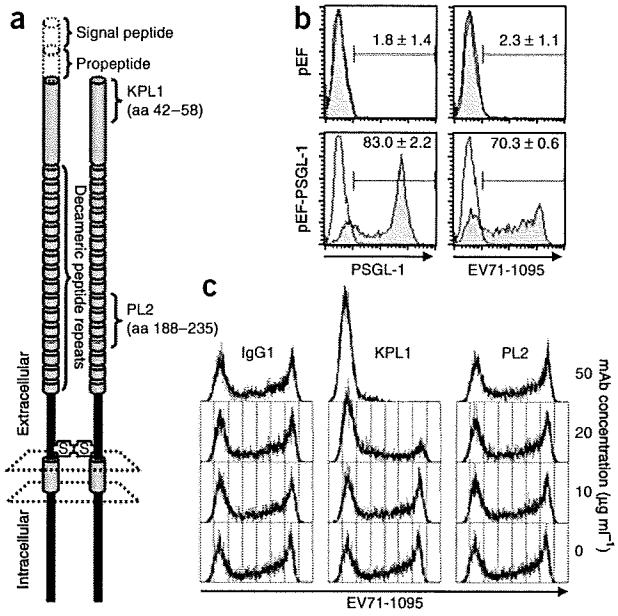

Figure 1 EV71-1095 binds human PSGL-1 expressed on 293T cells. (**a**) Schematic structure of human PSGL-1. The binding sites of PSGL-1–specific mAbs (KPL1 (ref. 14) and PL2 (ref. 15)) are indicated. aa, amino acids. (**b**) Flow cytometric analysis of 293T cells transfected with pEF-PSGL-1 or pEF (a control plasmid). Left, shaded and open areas represent staining with KPL1 mAb and isotype control, respectively. Right, shaded and open areas represent EV71-1095 binding assay and binding control with the mock-infected culture supernatant, respectively. The percentage of PSGL-1– or EV71-positive cells is indicated (mean ± s.d., $n = 3$). (**c**) EV71-1095 binding inhibition assay by flow cytometry. Dose-dependent inhibition of EV71-1095 binding to 293T cells transiently expressing PSGL-1 by mAb.

indicating PSGL-1–dependent EV71 replication in these cells. Furthermore, pretreatment of EV71-1095 with a soluble form of recombinant PSGL-1 (PSGL-1–Fc) impaired viral replication 2–4 d after viral inoculation of L-PSGL-1.1 cells (**Fig. 2e**) and RD cells (**Supplementary Table 2**) expressing undetectable PSGL-1 (data not shown), suggesting that the inhibitory effect of PSGL-1–Fc is due to either direct binding to EV71 virions or virion uncoating induced by the PSGL-1–Fc–EV71 interaction.

To elucidate the biological role of PSGL-1–dependent cell tropism of EV71-1095, we investigated the relationship between PSGL-1 expression on the cell surface (**Fig. 3a**) and replication of EV71 (**Fig. 3b**) in various cell lines (**Supplementary Table 2**). Among the four leukocyte cell lines examined, we found PSGL-1–dependent viral replication, as indicated by the reduction of viral titers in the presence of KPL1 in Jurkat T cells and U937 monocytic cells, which express large amounts of PSGL-1 on the cell surface. EV71-1095 induced a faint cytopathic effect in Jurkat T cells but no apparent cytopathic effect in the other leukocyte cell lines (data not shown). EV71-1095 replication was not affected by KPL1 in MT-2 cells and four nonleukocyte cell lines (RD, HEp-2c, SK-N-MC and Vero) that have little or no PSGL-1 expression, suggesting PSGL-1–independent replication through unidentified receptors in MT-2 and nonleukocyte cells. Taken together, these results suggest that EV71-1095 can use PSGL-1 as a functional cellular receptor in PSGL-1–positive leukocytes (**Supplementary Fig. 1a**), but it may use alternative mechanism(s) for replication in cells that have little or no PSGL-1 expression (**Supplementary Fig. 1b**).

Although the association of a specific genogroup with severe neurological diseases has not been identified through molecular epidemiological analyses of previous and recent EV71 isolates (genogroups A, B and C)[9,16], *in vitro* and *in vivo* phenotypes may be associated with certain amino acid determinants of EV71. Using eight representative EV71 strains (**Supplementary Table 1**), we investigated the strain specificity of EV71 and PSGL-1 use. We first examined the direct biochemical interaction between EV71 strains and PSGL-1–Fc by co-immunoprecipitation. The VP1 proteins of the SK-EV006, C7/Osaka, KED005, 1095 and 75-Yamagata strains of EV71 immunoprecipitated with PSGL-1–Fc (**Fig. 4a**). In contrast, the VP1 proteins of the BrCr, Nagoya and 02363 strains of EV71 did not immunoprecipitate with PSGL-1–Fc (**Fig. 4a**). Thus, these EV71 strains can be classified into two distinct phenotypes according to their PSGL-1–binding capability, regardless of genogroup: five PSGL-1–binding strains (EV71-PB; SK-EV006 (genogroup B3), C7/Osaka (B4), KED005 (C1), 1095 (C2) and 75-Yamagata (C4)) and three PSGL-1–nonbinding strains (EV71–non-PB; BrCr (A), Nagoya (B1) and 02363 (C1)). We then tested the PSGL-1–dependent replication competence of EV71-PB and EV71–non-PB strains in Jurkat T cells

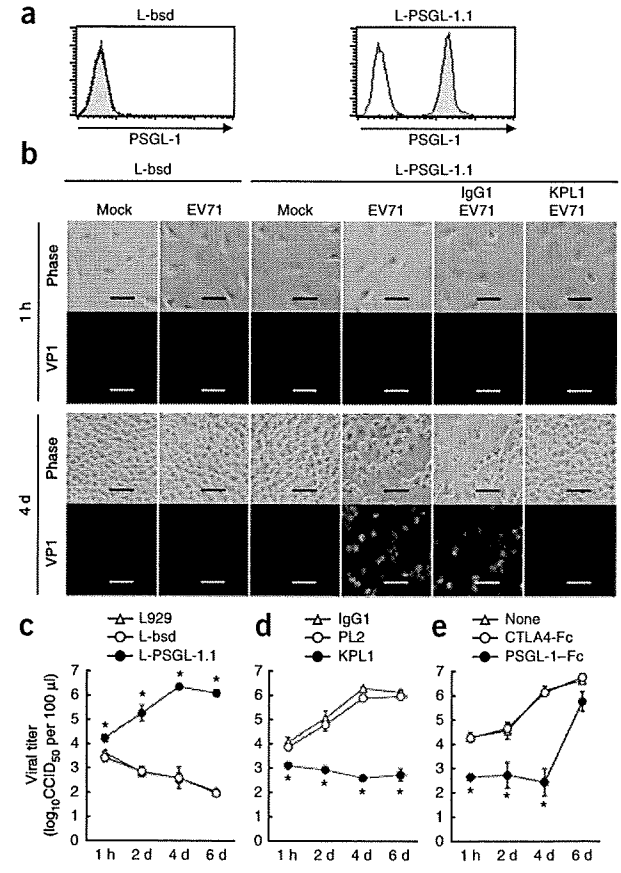

Figure 2 Stable expression of human PSGL-1 on mouse L929 cells permits infection by EV71-1095. (**a**) PSGL-1 expression on L-PSGL-1.1 and L-bsd (PSGL-1 negative control) cells, as measured by flow cytometry. (**b**) Development of cytopathic effect (Phase) and EV71 antigens by immunofluorescence (VP1). Scale bars, 100 μm. (**c**) Replication kinetics of EV71-1095 in L-PSGL-1.1 and PSGL-1–negative cells. (**d**) Replication kinetics of EV71-1095 in L-PSGL-1.1 cells in the presence of PSGL-1–specific (KPL1 and PL2) and control mAbs. (**e**) Replication kinetics of EV71-1095 in L-PSGL-1.1 cells after treatment with soluble PSGL-1. Viral titers and error bars are indicated as the means ± s.d. of triplicate analyses. Asterisks indicate $P < 0.01$ compared to the two controls.

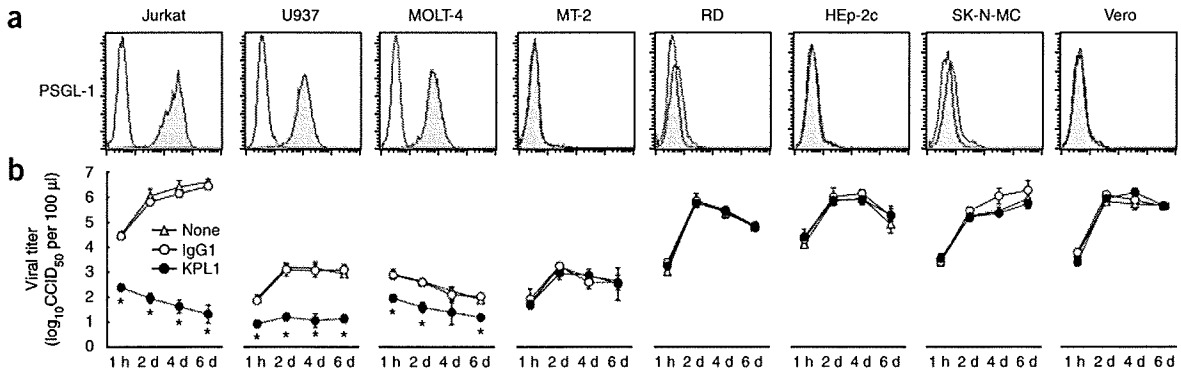

Figure 3 PSGL-1 expression and EV71-1095 replication kinetics in leukocyte and nonleukocyte cell lines. (**a**) PSGL-1 expression on the cell surface, as measured by flow cytometry. The shaded and open areas represent staining with PSGL-1–specific mAb (KPL1) and isotype control, respectively. (**b**) EV71-1095 replication kinetics in the presence of KPL1 and control mAbs. The titers and error bars are the means ± s.d. of triplicate analyses. Asterisks indicate $P < 0.01$ compared to the two controls.

(**Fig. 4b**). All five EV71-PB strains replicated in Jurkat T cells in a PSGL-1–dependent manner, as indicated by the reduction of viral titers in the presence of KPL1 at 4 d after inoculation (**Fig. 4b**). Among the three EV71–non-PB strains, two (Nagoya and 02363) replicated in Jurkat T cells in a PSGL-1–independent manner, and the BrCr strain replicated poorly (**Fig. 4b**). These data indicate that EV71-PB strains use PSGL-1 as the primary and functional receptor for infection of Jurkat T cells (**Supplementary Fig. 1a**), whereas some of the EV71–non-PB strains may use unidentified receptors for viral replication even in PSGL-1–positive T lymphocytes (**Supplementary Fig. 1c**). Although the KED005 and 02363 strains (genogroup C1) show distinct differences in their PSGL-1–binding phenotypes, only four amino acids (Ile55 of VP3 and Lys98, Glu145 and Ile262 of VP1 for the EV71-02363 strain) are different in the proteins comprising the entire capsid region of these two strains, suggesting that a few amino acid determinants in the capsid proteins are fully responsible for the phenotype (**Fig. 4**). Among the four amino acid differences, Glu145 of VP1 may be exposed on a surface-exposed loop in the capsid VP1 protein, and this has been identified as a major virulence determinant in mouse models[17,18].

We next investigated PSGL-1–dependent replication of the prototype CVA16-G10 strain. This strain replicated in L-PSGL-1.1 cells but not in L-bsd cells (a PSGL-1–negative control), and virus replication in L-PSGL-1.1 cells was inhibited by KPL1 (**Supplementary Fig. 4a,b**). The CVA16-G10 strain used PSGL-1 to infect L-PSGL-1.1 cells but not Jurkat T cells (**Supplementary Fig. 4c**), suggesting that CVA16-G10 represents a strain that uses an alternative entry mechanism via unidentified functional receptors for infection of Jurkat T cells.

PSGL-1 expressed on leukocytes has a crucial role in the tethering and rolling of leukocytes during recruitment of cells from blood vessels to the sites of acute inflammation upon stimulation by infection[2–4]. The tissue expression of PSGL-1 is primarily restricted to hematopoietic myeloid, lymphoid and dendritic lineages and to platelets. However, PSGL-1 is also expressed on the dendritic cells of lymph nodes and on macrophages in the intestinal mucosa[2], which could be the primary site of EV71 replication after viral ingestion. During the viremic phase of infection, a variety of circulating leukocytes expressing PSGL-1 may be responsible for the *in vivo* replication of EV71 (ref. 19) and subsequent EV71-induced apoptosis in the infected cells[12,20], possibly resulting in the T cell depletion and changes in cytokine levels observed in severe

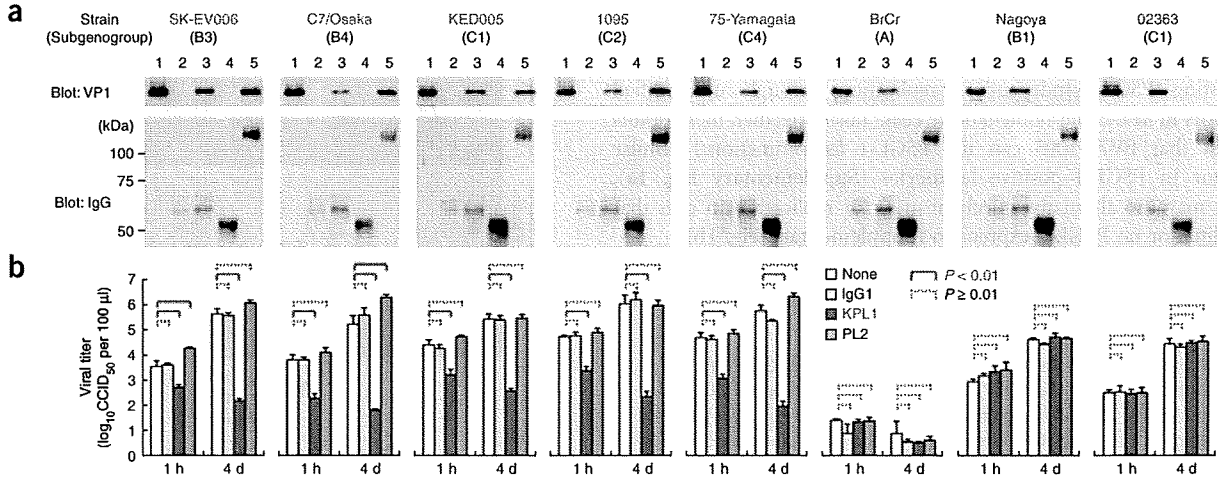

Figure 4 EV71 strain–specific binding to PSGL-1 and replication in Jurkat T cells. The strains that are EV71-PB and EV71–non-PB are indicated in red and blue, respectively. (**a**) Western blot showing the EV71 VP1 protein immunoprecipitated with PSGL-1–Fc. Concentrated viruses (lane 1) were incubated with isotype control mAb (lane 2), EV71-VP1–specific mAb (MA105, lane 3), negative control recombinant protein (CTLA4-Fc, lane 4) or PSGL-1–Fc (lane 5) and immunoprecipitated. (**b**) Viral replication in Jurkat T cells incubated with PSGL-1–specific (KPL1 and PL2) and control mAbs. Titers are expressed as the mean, and error bars indicate s.d. of triplicate analyses.

encephalitis cases with pulmonary edema[10,11]. In addition, the distribution and recruitment of PSGL-1–positive Langerhans cells and lymphocytes in inflamed skin[2] are consistent with the apparent HFMD pathogenesis associated with EV71 and CVA16 infection, which is characterized by acute skin inflammation. In this regard, our findings suggest the involvement of PSGL-1–positive inflammatory cells during the course of EV71 and CVA16 infection.

Although EV71 infects neurons and causes acute brainstem encephalitis, paralysis or both in humans[21,22] and experimental animals[17,23–25], PSGL-1 is apparently not expressed in the adult human brain[2]. Consistent with this observation, we have shown that EV71-1095 may also use PSGL-1–independent mechanism(s) for replication in nonleukocyte cells, including SK-N-MC neuroblastoma cells. Furthermore, CVA16, another causative agent of HFMD, can also use PSGL-1 as a functional receptor in L-PSGL-1.1 cells. Thus, PSGL-1–dependent viral replication is unlikely to be directly responsible for the neuronal cell apoptosis induced by EV71 (refs. 26,27). However, we cannot exclude the possible involvement of PSGL-1–positive inflammatory cells in the pathogenesis of HFMD and a variety of EV71 diseases with or without neurological manifestations.

We have shown that human PSGL-1 is a functional cellular receptor for EV71 infection. The occurrence of severe EV71 infection with a number of fatal encephalitis cases continues to be a major public health threat even now[28], but, currently, no vaccines or specific antiviral agents are available for EV71. Because soluble PSGL-1 inhibits EV71 replication, it may be a potential inhibitor of EV71-PB infection. The identification of PSGL-1 as a functional EV71 receptor on leukocytes is the first major step in elucidating EV71 pathogenesis at the molecular level. However, other EV71 and human enterovirus species A receptors on leukocyte and nonleukocyte cells may also have key implications in EV71 tropism and pathogenesis, particularly for severe central nervous system diseases. Further structural and functional analyses of interactions of EV71 with PSGL-1 and other unidentified receptors may provide new therapeutic approaches for the treatment of severe EV71 diseases.

METHODS

Methods and any associated references are available in the online version of the paper at http://www.nature.com/naturemedicine/.

Note: Supplementary information is available on the Nature Medicine website.

ACKNOWLEDGMENTS

We thank N. Takeda, S. Morikawa, Y. Matsuura, K. Moriishi, S. Koike, S. Yamayoshi and Y. Izumiya for helpful discussions; Y. Ami for technical advice regarding FACS; and N. Nishimura for preparing figures. We also thank M. Sinniah, M. Yusof (Institute for Medical Research, Malaysia) for providing EV71-SK-EV006 and KED005, N. Onnimala, Y. Pongsuwanna (National Institute of Health, Thailand) for providing EV71-02363, Y. Okuno (Osaka Prefectural Institute of Public Health) for providing EV71-C7/Osaka, K. Mizuta (Yamagata Prefectural Institute of Public Health) for providing EV71-75-Yamagata, A. Makino, Y. Tohya, H. Akashi (University of Tokyo) for providing P3U1 cells, H. Sakata (National Institute of Infectious Diseases, Japan) for providing L929 cells, and H. Shirato (National Institute of Infectious Diseases, Japan) for providing MOLT-4 and MT-2 cells. We are grateful to J. Wada for technical assistance. This work was supported by a Grant-in-Aid for Young Scientists from the Ministry of Education, Culture, Sports, Science and Technology, Japan (Y.N.). Y.N. and H.S. were supported in part by a Grant-in-Aid for Research on Emerging and Re-emerging Infectious Diseases and a Grant-in-Aid for the Promotion of Polio Eradication, from the Ministry of Health, Labour and Welfare, Japan.

AUTHOR CONTRIBUTIONS

Y.N. designed and performed experiments, analyzed data and wrote the paper; M.S. improved the expression cloning method; Y.T. prepared and characterized EV71-specific mAbs; and T.M. and T.W. analyzed data and wrote the paper. H.S. planned the project, designed experiments, analyzed data and wrote the paper. All authors discussed the results and commented on the manuscript.

Published online at http://www.nature.com/naturemedicine/
Reprints and permissions information is available online at http://npg.nature.com/reprintsandpermissions/

1. Rossmann, M.G., He, Y. & Kuhn, R.J. Picornavirus-receptor interactions. *Trends Microbiol.* **10**, 324–331 (2002).
2. Laszik, Z. *et al.* P-selectin glycoprotein ligand-1 is broadly expressed in cells of myeloid, lymphoid, and dendritic lineage and in some nonhematopoietic cells. *Blood* **88**, 3010–3021 (1996).
3. Sako, D. *et al.* Expression cloning of a functional glycoprotein ligand for P-selectin. *Cell* **75**, 1179–1186 (1993).
4. Somers, W.S., Tang, J., Shaw, G.D. & Camphausen, R.T. Insights into the molecular basis of leukocyte tethering and rolling revealed by structures of P- and E-selectin bound to SLe^X and PSGL-1. *Cell* **103**, 467–479 (2000).
5. Shimojima, M. *et al.* Usage of myeloma and panning in retrovirus-mediated expression cloning. *Anal. Biochem.* **315**, 138–140 (2003).
6. Oberste, M.S., Maher, K., Kilpatrick, D.R. & Pallansch, M.A. Molecular evolution of the human enteroviruses: correlation of serotype with VP1 sequence and application to picornavirus classification. *J. Virol.* **73**, 1941–1948 (1999).
7. Chan, L.G. *et al.* Deaths of children during an outbreak of hand, foot and mouth disease in Sarawak, Malaysia: clinical and pathological characteristics of the disease. *Clin. Infect. Dis.* **31**, 678–683 (2000).
8. Ho, M. *et al.* An epidemic of enterovirus 71 infection in Taiwan. *N. Engl. J. Med.* **341**, 929–935 (1999).
9. McMinn, P.C. An overview of the evolution of enterovirus 71 and its clinical and public health significance. *FEMS Microbiol. Rev.* **26**, 91–107 (2002).
10. Lin, T.Y., Hsia, S.H., Huang, Y.C., Wu, C.T. & Chang, L.Y. Proinflammatory cytokine reactions in enterovirus 71 infections of the central nervous system. *Clin. Infect. Dis.* **36**, 269–274 (2003).
11. Wang, S.M. *et al.* Pathogenesis of enterovirus 71 brainstem encephalitis in pediatric patients: roles of cytokines and cellular immune activation in patients with pulmonary edema. *J. Infect. Dis.* **188**, 564–570 (2003).
12. Chen, L.C. *et al.* Enterovirus 71 infection induces Fas ligand expression and apoptosis of Jurkat cells. *J. Med. Virol.* **78**, 780–786 (2006).
13. Snapp, K.R. *et al.* A novel P-selectin glycoprotein ligand-1 monoclonal antibody recognizes an epitope within the tyrosine sulfate motif of human PSGL-1 and blocks recognition of both P- and L-selectin. *Blood* **91**, 154–164 (1998).
14. Thatte, A. *et al.* Binding of function-blocking mAbs to mouse and human P-selectin glycoprotein ligand-1 peptides with and without tyrosine sulfation. *J. Leukoc. Biol.* **72**, 470–477 (2002).
15. Li, F. *et al.* Visualization of P-selectin glycoprotein ligand-1 as a highly extended molecule and mapping of protein epitopes for monoclonal antibodies. *J. Biol. Chem.* **271**, 6342–6348 (1996).
16. Brown, B.A., Oberste, M.S., Alexander, J.P. Jr., Kennett, M.L. & Pallansch, M.A. Molecular epidemiology and evolution of enterovirus 71 strains isolated from 1970 to 1998. *J. Virol.* **73**, 9969–9975 (1999).
17. Arita, M., Ami, Y., Wakita, T. & Shimizu, H. Cooperative effect of the attenuation determinants derived from poliovirus Sabin 1 strain is essential for attenuation of enterovirus 71 in the NOD/SCID mouse infection model. *J. Virol.* **82**, 1787–1797 (2008).
18. Chua, B.H., Phuektes, P., Sanders, S.A., Nicholls, P.K. & McMinn, P.C. The molecular basis of mouse adaptation by human enterovirus 71. *J. Gen. Virol.* **89**, 1622–1632 (2008).
19. Kung, C.M. *et al.* Differences in replication capacity between enterovirus 71 isolates obtained from patients with encephalitis and those obtained from patients with herpangina in Taiwan. *J. Med. Virol.* **79**, 60–68 (2007).
20. Kuo, R.L., Kung, S.H., Hsu, Y.Y. & Liu, W.T. Infection with enterovirus 71 or expression of its 2A protease induces apoptotic cell death. *J. Gen. Virol.* **83**, 1367–1376 (2002).
21. Hsueh, C. *et al.* Acute encephalomyelitis during an outbreak of enterovirus type 71 infection in Taiwan: report of an autopsy case with pathologic, immunofluorescence and molecular studies. *Mod. Pathol.* **13**, 1200–1205 (2000).
22. Wong, K.T. *et al.* The distribution of inflammation and virus in human enterovirus 71 encephalomyelitis suggests possible viral spread by neural pathways. *J. Neuropathol. Exp. Neurol.* **67**, 162–169 (2008).
23. Nagata, N. *et al.* Pyramidal and extrapyramidal involvement in experimental infection of cynomolgus monkeys with enterovirus 71. *J. Med. Virol.* **67**, 207–216 (2002).
24. Nagata, N. *et al.* Differential localization of neurons susceptible to enterovirus 71 and poliovirus type 1 in the central nervous system of cynomolgus monkeys after intravenous inoculation. *J. Gen. Virol.* **85**, 2981–2989 (2004).
25. Ong, K.C. *et al.* Pathologic characterization of a murine model of human enterovirus 71 encephalomyelitis. *J. Neuropathol. Exp. Neurol.* **67**, 532–542 (2008).
26. Chang, S.C., Lin, J.Y., Lo, L.Y.C., Li, M.L. & Shih, S.R. Diverse apoptotic pathways in enterovirus 71–infected cells. *J. Neurovirol.* **10**, 338–349 (2004).
27. Chen, C.S. *et al.* Retrograde axonal transport: a major transmission route of enterovirus 71 in mice. *J. Virol.* **81**, 8996–9003 (2007).
28. World Health Organization. Outbreak news. Enterovirus, China. *Wkly. Epidemiol. Rec.* **83**, 169–170 (2008).

ONLINE METHODS

Cells. L929 cells were generously provided by H. Sakata P3U1 cells were generously provided by H. Akashi. 293T cells were generously provided by Y. Matsuura. GP2-293 cells were obtained from Clontech. Jurkat cells were obtained from Riken Cell Bank. U937 cells were obtained from the Japanese Collection of Research Biosources. MOLT-4 and MT-2 cells were generously provided by H. Shirato. RD cells were obtained from the US Centers for Disease Control. HEp-2 cells were obtained from the Victorian Infectious Diseases Reference Laboratory. SK-N-MC cells were obtained from DS Pharma Biomedical. Vero cells were obtained from Japan Poliomyelitis Research Institute. We cultured L929, 293T and GP2-293 cells in DMEM (Sigma) supplemented with 10% FCS. We maintained P3U1, Jurkat, U937, MOLT-4 and MT-2 cells in RPMI-1640 medium (Sigma) with 10% FCS. We maintained RD, HEp-2c, SK-N-MC and Vero cells in Eagle's minimal essential medium (Nissui) supplemented with 10% FCS.

Viruses. We propagated all EV71 strains (**Supplementary Table 1**) in RD or Vero cells. Because some of the strains produced diffuse plaques on RD cells, we determined the viral titers by a microtitration assay using 96-well plates and RD cells as previously described[23]. Briefly, we used ten wells for each viral dilution and expressed the viral titers as 50% cell culture infectious dose ($CCID_{50}$).

Monoclonal antibodies and recombinant proteins. We generated the EV71-specific mAbs MA105 (mouse IgG2b) and MA35 (mouse IgG2a) from mice immunized with EV71-1095 (Y. Tano *et al.*, unpublished data). We purchased the EV71-specific mAb 10F0 from Biogenesis. We purchased the mAbs to human CD34 (clone 563), human CD43 (L60), human PSGL-1 (KPL1), and mouse Psgl-1 (4RA10) from BD Biosciences, and we purchased human PSGL-1–specific mAb PL2 from Beckman-Coulter. For negative controls, we purchased human (MOPC-21) and rat IgG1 (R3-34) and human IgG2b (27-35) from BD Biosciences. We used NaN_3-free mAbs, MOPC-21 (BioLegend) and NCG01 (Lab Vision) in cell culture as negative controls. We purchased soluble recombinant forms of human proteins fused to the Fc region of human IgG1 (PSGL-1–Fc and cytotoxic T lymphocyte antigen-4–Fc) from R&D Systems.

Preparation of EV71-1095–coated dishes and selection of Jurkat T cell clones. We incubated a polystyrene Petri dish (Ina-optika) with 10 μg ml^{-1} MA35 in 10 ml of 50 mM Tris-HCl (pH 9.4) at 4 °C overnight. We rinsed the dishes twice with PBS containing 2% FCS (PBS-2FCS) and blocked them with PBS-2FCS at 25 °C for 30 min. We then applied EV71-1095 (10 ml, $1 \times 10^{8.6}$ $CCID_{50}$ ml^{-1}) to the MA35-coated dishes and incubated at 25 °C for 30 min. We replaced the supernatant with a fresh viral preparation, and we repeated replacing the supernatant three times. We fixed the dishes with a viral preparation containing 1% paraformaldehyde for 30 min at 25 °C. Finally, we washed the dishes with PBS-2FCS five times and used them for selection and expression cloning.

We selected Jurkat T cell clones that expressed high levels of EV71-binding molecules on the cell surface with the panning method with EV71-1095–coated dishes. We added Jurkat T cells to the EV71-coated dishes in RPMI-1640 medium and incubated them at 4 °C for 90 min. We removed nonadherent cells by washing with RPMI-1640 medium, and we cultured the adherent cells for a week. We used the Jurkat T cell colonies on the EV71-coated dishes for preparation of the cDNA library.

Retroviral cDNA library. Using the Jurkat T cell colonies on the EV71-coated dishes, we prepared a retroviral cDNA library as previously described[29] with minor modifications. We used the Pantropic Retroviral Expression System (Clontech) to prepare vesicular stomatitis virus G protein–pseudotyped retroviruses. We ligated the Jurkat cDNA with the EcoRI adaptor and cloned it into the EcoRI site of the pLIB retroviral vector (Clontech). We transfected the pLIB plasmid along with a vesicular stomatitis virus G protein expression plasmid into GP2-293 cells with Lipofectamine 2000 (Invitrogen). We harvested the culture supernatant 2 d after transfection and used it to infect P3U1 cells.

Expression cloning of the EV71-binding receptor. We preformed retrovirus-mediated expression cloning using EV71-coated dishes and P3U1 cells as described previously[5]. We isolated genomic DNA from each P3U1 cell colony bound to the EV71-coated dishes, subjected it to PCR amplification with pLIB-specific primers and sequenced the amplification product.

Expression plasmids. We cloned the cDNAs encoding human *SELPLG*, *CD34*, *SPN* and mouse *Selplg* into pEF6-Flag-3S to produce pEF-PSGL-1, pEF-CD34, pEF-CD43 and pEF-mPsgl-1, respectively. For hmPSGL-1 expression, we constructed chimeric *SELPLG* cDNA by PCR and cloned it into pEF6-Flag-3S. The primers used for cDNA cloning and chimeric protein construction and mutation are shown in **Supplementary Tables 3** and **4**. More details are provided in the **Supplementary Methods**.

Detection of cell surface molecules by flow cytometry. We washed cells once with flow cytometry buffer (PBS supplemented with 2 mM EDTA, 2% FCS and 0.1% NaN_3) and incubated them with mAb on ice for 30 min. After washing with flow cytometry buffer, we incubated the cells with secondary antibodies conjugated to Alexa Fluor 488 (Invitrogen). We washed and analyzed the cells by FACSCalibur (BD Biosciences).

EV71-binding assay by flow cytometry. We collected 293T cells 24 h after transfection with expression plasmids, washed them once with flow cytometry buffer and incubated them with the EV71-1095 preparation (1×10^7 $CCID_{50}$) supplemented with 0.1% NaN_3 or concentrated viruses (containing 0.5 μg of VP1 protein) per 50 μl flow cytometry buffer. In the binding inhibition assay with mAbs, we treated cells with mAb for 30 min on ice before exposing them to the virus. We washed the cells and stained them with Alexa Fluor 488–conjugated MA105, washed them and then analyzed them by FACSCalibur.

Establishment of the L-PSGL-1.1 cell line. To establish a mouse L929 cell line expressing human PSGL-1, we transfected L929 cells with pEF-PSGL-1 and selected stable transfectants with 5 μg ml^{-1} blasticidin S HCl (Invitrogen). Through a limiting dilution of the various cell colonies, we selected three of the 16 cell lines on the basis of high PSGL-1 expression. Finally, we established L-PSGL-1.1 as the single cell clone that supported the most efficient EV71-1095 replication. As a PSGL-1–negative control, we also established an L-bsd cell line by transfecting L929 cells with pEF6-Flag-3S followed by selection with 5 μg ml^{-1} blasticidin.

Immunofluorescence microscopy. We fixed cells with 4% paraformaldehyde in PBS for 30 min at 25 °C, washed them, permeabilized them with PBS containing 1% Triton X-100 for 10 min at 25 °C, blocked them with PBS containing 1% BSA for 10 min at 25 °C and incubated them with VP1-specific mAb 10F0 labeled with Alexa Fluor 488 for 30 min at 37 °C. After a final wash, we analyzed the cells with a fluorescence microscope (Keyence).

Immunoprecipitation and western blotting. We diluted concentrated viruses (0.5 μg VP1 protein) in 300 μl of immunoprecipitation buffer (20 mM Tris-Cl, 135 mM NaCl, 1% Triton X-100 and 10% glycerol; pH 7.4) and incubated them with 1 μg of mAb or chimeric proteins for 2 h at 4 °C. We added Dynabeads Protein G (Invitrogen) and incubated the mixture for an additional 2 h. We washed the beads and subjected the immunoprecipitates to 12.5% SDS-PAGE. For western blotting, we transferred the proteins onto nitrocellulose membranes and blotted with MA105.

Viral infection assays. We inoculated cells (4×10^4 cells per 200 μl in a 48-well plate) with viruses at 10 $CCID_{50}$ per cell for 1 h, washed them and incubated them in medium at 34 °C (for L-PSGL-1.1, Jurkat, U937, MOLT-4 or MT-2 cells) or 37 °C (for RD, HEp-2c, SK-N-MC or Vero cells). For mAb inhibition, we pretreated the cells with 10 μg ml^{-1} mAb for 1 h, washed them and maintained them in the medium with 10 μg ml^{-1} mAb. For inhibition with PSGL-1–Fc, we pretreated EV71-1095 (1×10^5 $CCID_{50}$) with 1 μg PSGL-1–Fc per 100 μl for 1 h and then inoculated them into L-PSGL-1.1 cells. We incubated the cells for 1 h in the presence of PSGL-1–Fc, washed them and maintained them in the absence of PSGL-1–Fc. We subjected the culture supernatants and infected cells to three cycles of freeze-thawing before titration.

Statistical analyses. We carried out all infection assays in triplicate and compared the mean viral titers with Student's *t* test (two-tailed). We considered *P* values of <0.01 statistically significant.

29. Kitamura, T. & Morikawa, Y. Isolation of T-cell antigens by retrovirus-mediated expression cloning. *Methods Mol. Biol.* **134**, 143–152 (2000).

JOURNAL OF VIROLOGY, Mar. 2009, p. 2510–2517 Vol. 83, No. 6
0022-538X/09/$08.00+0 doi:10.1128/JVI.02416-08

Mitogen-Activated Protein Kinase-Activated Kinase RSK2 Plays a Role in Innate Immune Responses to Influenza Virus Infection▽

Satoshi Kakugawa,[1] Masayuki Shimojima,[1] Hideo Goto,[1] Taisuke Horimoto,[1] Naoki Oshimori,[3] Gabriele Neumann,[5] Tadashi Yamamoto,[3] and Yoshihiro Kawaoka[1,2,4,5]*

Division of Virology, Department of Microbiology and Immunology, Institute of Medical Science, University of Tokyo, 4-6-1 Shirokanedai, Minato-ku, Tokyo 108-8639, Japan[1]; Exploratory Research for Advanced Technology (ERATO), Japan Science and Technology Agency, Saitama 332-0012, Japan[2]; Division of Oncology, Institute of Medical Science, University of Tokyo, 4-6-1 Shirokanedai, Minato-ku, Tokyo 108-8639, Japan[3]; International Research Center for Infectious Diseases, Institute of Medical Science, University of Tokyo, Tokyo 108-8639, Japan[4]; and Department of Pathobiological Sciences, School of Veterinary Medicine, University of Wisconsin, Madison, Wisconsin 53706[5]

Received 24 November 2008/Accepted 29 December 2008

Viral infections induce signaling pathways in mammalian cells that stimulate innate immune responses and affect cellular processes, such as apoptosis, mitosis, and differentiation. Here, we report that the ribosomal protein S6 kinase alpha 3 (RSK2), which is activated through the "classical" mitogen-activated protein kinase pathway, plays a role in innate immune responses to influenza virus infection. RSK2 functions in the regulation of cell growth and differentiation but was not known to play a role in the cellular antiviral response. We have found that knockdown of RSK2 enhanced viral polymerase activity and growth of influenza viruses. Influenza virus infection stimulates NK-κB- and beta interferon-dependent promoters. This stimulation was reduced in RSK2 knockdown cells, suggesting that RSK2 executes its effect through innate immune response pathways. Furthermore, RSK2 knockdown suppressed influenza virus-induced phosphorylation of the double-stranded RNA-activated protein kinase PKR, a known antiviral protein. These findings establish a role for RSK2 in the cellular antiviral response.

Influenza A viruses cause highly contagious respiratory infections in humans and several animal species (reviewed in reference 51). Annual epidemics account for an estimated 20,000 excess deaths and 100,000 excess hospitalizations in the United States alone. Pandemics occur at irregular intervals and can claim millions of lives, as witnessed with the "Spanish influenza" in 1918 and 1919, which killed an estimated 40 to 50 million people worldwide.

Influenza A viruses belong to the family *Orthomyxoviridae* and possess eight segments of single-stranded, negative-sense RNA, which encode 10 or 11 proteins (reviewed in reference 36). Four viral proteins—the polymerase subunits PB2, PB1, and PA and the nucleoprotein NP—are required for the replication and transcription of the viral RNA (vRNA). Two viral surface glycoproteins (hemagglutinin and neuraminidase [NA]) are critical for virus binding and release and are the major viral antigens. The NS1 protein is a multifunctional factor that counteracts the cellular interferon (IFN) responses that are triggered upon influenza virus infection (4, 9, 12, 21, 29, 30, 48, 49). Other viral proteins play a critical role(s) in the nuclear export of newly synthesized viral replication complexes (i.e., the matrix protein M1 and the nuclear export protein NS2), virus entry (i.e., the ion channel protein M2), and the regulation of apoptosis (i.e., the PB1-F2 protein, which is not encoded by all influenza A virus strains); the functions of these proteins are described in detail in reference 36.

Stimuli such as stress, cytokines, mitogens, and viral infections trigger multiple signaling cascades, such as the mitogen-activated protein kinase (MAPK) pathways, in mammalian cells (reviewed in references 10, 40, and 41). MAPK signaling pathways regulate critical cellular activities, such as gene expression, metabolism, apoptosis, mitosis, and differentiation. In the "classical" MAPK pathway, Raf-1 (a serine/threonine kinase) activates MEK1/2 (a MAPK kinase kinase), which subsequently activates the MAPK kinase extracellular signal-regulated kinases 1 and 2 (ERK1/2). In addition to ERK1/2, several other MAPK family members have been identified in mammalian cells, including p38 isoforms, c-Jun amino-terminal kinases, and BMK/ERK5 (big MAPK). MAPKs can activate their targets through direct phosphorylation or through the phosphorylation of downstream kinases (MAPK-activated protein kinases). Prominent examples of MAPK-activated protein kinases are p90 ribosomal S6 kinases (RSKs), which have emerged as major downstream mediators of ERK signal transduction (reviewed in references 6 and 41). In mammals, four RSKs (RSK1 to -4) have been identified; these are ubiquitously expressed and promote cell growth, proliferation, and cell survival (the last by interfering with apoptotic effectors). Despite their role as downstream mediators of ERK signal transduction, RSKs were not previously known to have antiviral effects.

Influenza virus infection has been shown to activate all known MAPK pathways (reviewed in references 26 and 27). Influenza virus-induced activation of the p38 and c-Jun amino-terminal kinase pathways seems to trigger antiviral effects (23,

* Corresponding author. Mailing address: Division of Virology, Department of Microbiology and Immunology, Institute of Medical Science, University of Tokyo, 4-6-1 Shirokanedai, Minato-ku, Tokyo 108-8639, Japan. Phone: 81-3-5449-5310. Fax: 81-3-5449-5408. E-mail: kawaoka@ims.u-tokyo.ac.jp.

▽ Published ahead of print on 7 January 2009.

25), while activation of the ERK1/2 and big MAPK pathways likely supports influenza virus replication (39). Further studies are needed to establish the significance of these signaling pathways for influenza virus replication.

Influenza virus infection also activates the IκB kinase/NF-κB pathway (reviewed in reference 19). This pathway is activated by a number of other viruses and leads to the expression of proinflammatory and antiviral cytokines, including beta IFN (IFN-β) and tumor necrosis factor alpha. The role of NF-κB activation in the context of influenza virus infection is still unclear, as two studies found a virus-supportive role (32, 50) and another study suggested that NF-κB activation is not required for efficient influenza virus replication (5).

In this study, we provide evidence that the MAPK-activated protein kinase ribosomal protein S6 kinase alpha 3 (RSK2) is activated upon influenza virus infection and that this kinase affects antiviral responses through NF-κB, IFN-β, and a known antiviral factor, PKR. These findings establish a novel antiviral role for RSK2.

MATERIALS AND METHODS

Cell culture. Human embryonic kidney cells (293T cells and 293 cells) were cultured in Dulbecco's modified Eagle's medium (DMEM; Sigma) supplemented with 10% heat-inactivated fetal calf serum (FCS) and antibiotics. Plat-GP (murine leukemia virus-based packaging) cells were kindly provided by T. Kitamura (University of Tokyo, Tokyo, Japan) and cultured in DMEM with 10% FCS and 10 μg/ml blasticidin (Invitrogen). QT6 quail fibrosarcoma cells were maintained in Ham's F-12K medium (MP Biomedicals) supplemented with 10% FCS and 10% tryptose phosphate broth (Sigma). Madin-Darby canine kidney (MDCK) cells were cultured in minimal essential medium containing 5% newborn calf serum and antibiotics.

Viruses. PB2-627K- and PB2-627E-expressing influenza viruses were generated by reverse genetics (31) and propagated in MDCK cells. Both viruses possess the hemagglutinin and NA genes of A/WSN/33 (H1N1) virus, while the remaining genes were derived from A/Hong Kong/483/97 (H5N1) virus; the PB2 protein of this virus possesses a lysine at position 627, resulting in PB2K virus. PB2E virus is a derivative that possesses glutamic acid at position 627 in the PB2 protein. Influenza virus B/Hong Kong/73 and Sendai virus (Enders strain; kindly provided by Allan Portner, St. Jude Children's Research Hospital, Memphis, TN) were also propagated in MDCK cells. Viruses were titrated by plaque assay in MDCK cells.

Plasmids. The PB1, PA, and NP proteins of A/Hong Kong/483/97 (H5N1) virus were expressed with the pMX vector (34), which was kindly provided by T. Kitamura, University of Tokyo, Tokyo, Japan. For the PB2 protein, we used a variant that possesses glutamic acid at position 627 (PB2E). pPolI-fCD2 and pPolI-Luc drive the synthesis of negative-sense vRNAs comprising the 3′ noncoding region of the NA (A/Hong Kong/483/97) vRNA, the complementary coding sequence of luciferase or feline CD2 (fCD2) (45), respectively, and the 5′ noncoding region of the NA vRNA.

Gallus gallus RSK2 and human PKR were cloned from chicken embryo fibroblasts or human 293T cells, as appropriate. Briefly, RNA was extracted from these cells by use of the RNeasy minikit (Qiagen). Reverse transcription-PCR was performed with an oligo(dT) primer followed by PCR with gene-specific primers. The PCR products were cloned into the pCAGGS vector (under the control of the chicken β-actin promoter [33]) and then sequenced. To escape the knockdown effect of the short hairpin RNA (shRNA), a silent mutation was introduced into the human RSK2 protein expression plasmid, yielding pmRSK2.

pNF-κB-Luc, which expresses luciferase upon promoter activation by NF-κB, was purchased from Stratagene. pIFN-luc, which express luciferase under the control of an IFN-β-dependent promoter, was derived from the following components: the bacterial artificial chromosome clone RP11-113D19, which was used as the source of the promoter and terminator regions of the human IFN-β gene (Invitrogen), and pGEM-luc (Promega), which was used as the source of the luciferase gene. These components were joined by PCR, and the resulting construct was cloned into the pUC19 vector.

cDNA library. A cDNA library was prepared from quail QT6 cells by isolating mRNA (with the FastTrack 2.0 mRNA isolation kit; Invitrogen). cDNA was synthesized by use of the SuperScript Choice system for cDNA synthesis (Invitrogen), according to the manufacturer's instructions. The resulting cDNAs were size fractionated by agarose gel electrophoresis, and cDNA fragments longer than 1 kbp were extracted from the gel with the Qiaex II gel extraction kit (Qiagen). The respective cDNA fragments were then inserted into the BstXI sites of pCAGGS-Kan (a pCAGGS variant that carries the kanamycin resistance gene) by using BstXI adapters (Invitrogen). The ligated DNA was ethanol precipitated and then electroporated into DH10B competent cells.

Library screening. Human embryonic kidney 293T cells were transfected with plasmids for the expression of the polymerase and NP proteins, i.e., pMX-PB2E (possessing glutamic acid at position 627), -PB1, -PA, -NP; with the plasmid for the synthesis of a virus-like RNA encoding fCD2 (polI-fCD2); and with the quail QT6 cDNA library. Cells were incubated for 2 days at 33°C, collected, and treated with an antibody against fCD2 (44, 45). After incubation at 4°C for 30 min, fCD2-positive cells were selected by immunoaffinity with Bio-Adembeads goat anti-mouse immunoglobulin M (IgM) antibody (Ademtech) according to the manufacturer's instructions. Plasmid DNA was then extracted from the cells and amplified in *Escherichia coli* in Luria-Bertani medium supplemented with kanamycin. Selection of cells that expressed high levels of fCD2 was repeated four times, at which point plasmid DNA was extracted from the cells and sequenced.

Luciferase assay. Luciferase assays were performed by use of a dual-luciferase reporter assay system (Promega) on a microplate luminometer (Veritas; Turner Biosystems, Sunnyvale, CA), according to the manufacturer's instructions. As an internal control for the dual-luciferase assay, pGL4.74[hRluc/TK] (Promega) was used.

Construction of RSK2 knockdown cells by use of a retroviral vector. shRNA with a human RSK2 target sequence (5′-GATGCTGCTTGTGATATATGG-3′) was flanked by the mU6 promoter and terminator. The resulting cDNA was inserted into the pSSSP vector, which was kindly provided by H. Iba (University of Tokyo, Tokyo, Japan). A similar plasmid, pSSSP-shGFP, with a target sequence for green fluorescent protein (GFP) (5′-GCCACAACGTCTATATCA TGG-3′) was also kindly provided by H. Iba (University of Tokyo, Tokyo, Japan). These plasmids were used to produce murine leukemia virus-based viruses in Plat-GP cells, as described previously (20, 45), and then used to transduce 293 cells.

Analysis of virus propagation. To establish virus growth rates, three wells of cells were infected in parallel with virus at a multiplicity of infection (MOI) of 0.05 and incubated at 33°C or 37°C. At various times, supernatants were assayed to determine the titer of the infectious virus by plaque assay of MDCK cells.

NF-κB and IFN-β promoter activity. pNF-κB-Luc and pIFN-luc were transfected into 293 (human embryonic kidney) cells with a retroviral vector expressing shRNA specific to human RSK2 (shRSK2 cells) and shGFP cells, respectively. Nine hours later, cells were infected with virus at an MOI of 1.0 and incubated at 33°C. Twelve hours later, the levels of luciferase expression were determined.

Western blot analysis. To assess RSK2 expression levels, shRSK2 cells and shGFP cells were suspended in Tris-glycine sodium dodecyl sulfate (SDS) sample buffer (Invitrogen), and Western blot analysis was performed with anti-RSK2 (E1; Santa Cruz Biotechnology) and anti-β-actin (as an internal control; Sigma) antibodies, according to the manufacturers' instructions. Biotinylated anti-mouse IgG antibody (Vector) was used as a secondary antibody. Bands were detected with the Vectastain ABC kit (Vector) and ECL Plus Western blotting detection reagents (GE Healthcare); the VersaDoc imaging system (Bio-Rad) was used to quantify band intensities.

To analyze expression of the viral M1 protein, shRSK2 cells and control shGFP cells were infected with a PB2-627E-expressing virus at an MOI of 1.0 and incubated at 33°C. At various times, the cells were washed three times with phosphate-buffered saline and resuspended in Tris-glycine SDS sample buffer. Western blot analysis was performed with monoclonal antibodies specific to the M1 protein, with β-actin as a control. Biotinylated anti-mouse IgG antibody (Vector) was used as a secondary antibody. Bands were detected as described above.

To assess RSK2 phosphorylation levels, 293 cells (7.5×10^5 cells) were plated in 60-mm plates and cultured overnight at 37°C. The growth medium was replaced with DMEM containing 4% bovine serum albumin, and cells were infected with influenza virus (MOI of 3.0) 12 hours later; control cells remained uninfected. Three hours postinfection, RSK2 was immunoprecipitated with anti-RSK2 antibody (E1; Santa Cruz) coupled to protein G beads. The beads were resuspended in Tris-glycine SDS sample buffer, and Western blot analysis was performed with antibodies specific for RSK phosphorylated at Thr365/Ser369, Ser386, or Thr577 (antibodies obtained from Cell Signaling). Biotinylated anti-rabbit IgG antibody (Vector) was used as a secondary antibody. Bands were detected as described above.

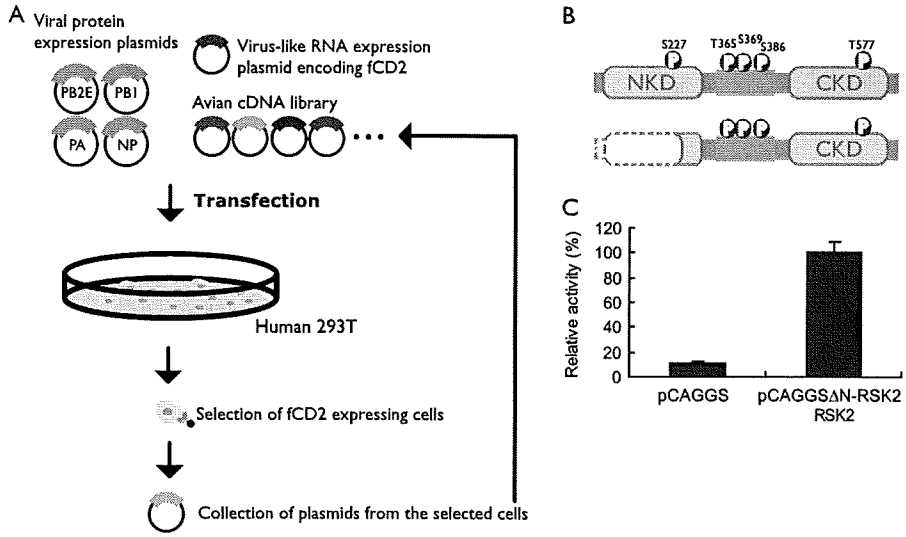

FIG. 1. Identification of cellular proteins that enhance influenza virus replication and downregulation of influenza virus replication by RSK2. (A) Human embryonic kidney 293T cells were transfected with plasmids encoding the components of the influenza viral replication complex (PB2, PB1, PA, and NP). The PB2 protein possesses glutamic acid at position 627 (PB2-627E), which supports efficient replication in avian cells but not in mammalian cells at 33°C. Cells were cotransfected with a plasmid for the synthesis of a virus-like RNA encoding fCD2 (polI-fCD2) and with an avian (quail cell) cDNA library. Cells expressing avian proteins that support efficient replication by PB2-627E virus in mammalian cells at 33°C will produce increased amounts of fCD2. Cells with high levels of fCD2 were selected by immunoaffinity using anti-fCD2 antibody. After a total of four rounds of selection, plasmid DNA was extracted from the cells and sequenced. (B) Schematic diagram of human RSK2 (top) and the N-terminally deleted avian RSK2 protein selected in our screening approach (bottom). The CKD is activated by ERK1/2, resulting in the activation of the NKD. The NKD subsequently phosphorylates target proteins. (C) Influenza viral polymerase activity in 293T cells expressing avian ΔN-RSK2. Cells were transfected with plasmids expressing PB2E, PB1, PA, and NP; a virus-like RNA encoding luciferase (pPolI-luc); and the N-terminally deleted avian RSK2 protein (pCAGGS-ΔN-RSK2) or the "empty" control vector (pCAGGS). Cells were maintained at 33°C for 24 h and were then subjected to luciferase assays. In human cells at 33°C, expression of N-terminally deleted avian RSK2 increased the activity of a replication complex possessing glutamic acid at position 627 in the PB2 protein. The error bars represent standard deviations from three independent experiments.

To assess the phosphorylation levels of PKR, shRSK2 and control shGFP cells were infected at an MOI of 0.01 or 1.0 with influenza virus and incubated at 33°C. Infected cells were collected at 0, 6, and 12 h postinfection. Western blot analysis was performed with anti-PKR (Santa Cruz), anti-phospho-PKR (Biosource), and anti-β-actin (as an internal control; Sigma) antibodies according to the manufacturers' instructions. Biotinylated anti-rabbit IgG antibody or anti-mouse IgG antibody was used as a secondary antibody. Bands were detected as described above.

Statistical analysis. Student's *t* test was used to determine statistical significance.

RESULTS AND DISCUSSION

Relatively little is known about the host factors that interact with influenza virus components. The influenza virus PB2 protein is now recognized as a critical determinant of pathogenicity and host range restriction (16, 17, 28, 46, 47). In general, lysine 627 of the PB2 protein confers a high level of pathogenicity to influenza viruses in mammals (16), which can be modeled by efficient replication in mammalian cells at 33°C and 37°C (17). In contrast, viruses with a glutamic acid residue at this position (PB2-627E) have low pathogenicity in mammals (16) and attenuated virus replication in mammalian systems at 33°C and, to a lesser extent, at 37°C (17). In order to identify the host factor(s) that restricts PB2-627E virus growth in mammalian cells, we transfected human embryonic kidney (293T) cells with a plasmid for synthesis of an influenza virus-like RNA. This virus-like RNA encodes fCD2; fCD2 thus serves as a reporter protein (45) to assess viral replication efficiencies. We cotransfected cells with plasmids for expression of the A/Hong Kong/483/97 (H5N1) virus NP, PB1, and PA proteins and a plasmid for expression of a mutant PB2, PB2-627E (Fig. 1A). The PB2-627E mutation restricts amplification of the virus-like RNA in human cells at 33°C. To identify the avian host factor(s) that "rescues" efficient replication, even with PB2-627E, we cotransfected human 293T cells with a cDNA expression library derived from avian quail QT6 cells. Avian host factors that mediate efficient replication of PB2-627E virus should support high levels of fCD2 expression from the virus-like RNA. The fCD2-positive cells were selected with an antibody against fCD2. After four rounds of selection, we extracted plasmids from the fCD2-positive transfectants and subjected them to sequencing.

One of the identified host proteins was the quail homolog of the *Gallus gallus* RSK2, from which 310 N-terminal amino acids were missing (avian ΔN-RSK2) (Fig. 1B). To confirm that avian ΔN-RSK2 enhances influenza virus replication in mammalian cells at 33°C, we overexpressed this protein in human cells that expressed the viral replication complex components (i.e., PB2-627E, PB1, PA, and NP) and a virus-like RNA that encodes the luciferase reporter protein. Our results indicate that luciferase expression was elevated in cells expressing avian ΔN-RSK2 protein relative to that in control cells expressing the "empty" expression vector (Fig. 1C).

Next, we cloned the full-length avian and human RSK2 proteins and tested their ability to enhance PB2-627E-mediated replication in human cells at 33°C; however, we did not detect a significant effect for either protein (data not shown).

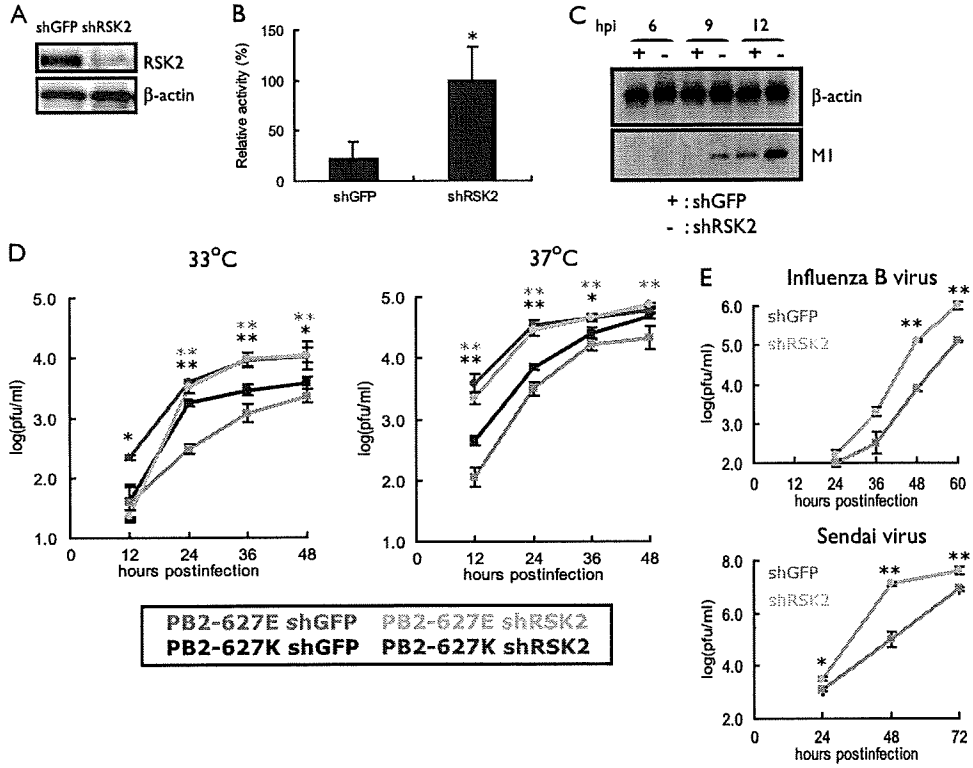

FIG. 2. Effect of RSK2 knockdown on influenza virus replication. (A) Knockdown of human RSK2. 293 cells were transduced with retroviral vectors for shRNAs to human RSK2 or GFP (as a control), resulting in shRSK2 and shGFP cells. RSK2 expression levels were assessed by Western blotting with an antibody to this protein. β-Actin expression levels served as an internal control. (B) Viral polymerase activity in shRSK2 and shGFP cells. Cells were transfected with plasmids that directed synthesis of PB2-627E, PB1, PA, NP, and pPolI-luc. After incubation at 33°C for 24 h, cell lysates were prepared and subjected to luciferase assays. Knockdown of RSK2 resulted in more-efficient replication of the virus-like RNA, suggesting that RSK2 suppresses influenza virus replication. The error bars represent standard deviations from three independent experiments. The statistical significance of the difference between the control and test samples is shown by the P value, which was determined by Student's t test (*, $P < 0.05$). (C) Viral protein production in shRSK2 cells and shGFP cells. shRSK2 and shGFP cells were infected with virus possessing PB2-627E and incubated at 33°C. At the indicated time points postinfection, Western blot analysis was carried out with antibodies against M1 and β-actin. (D) Influenza A virus growth in shRSK2 cells. shRSK2 and control shGFP cells were infected at an MOI of 0.05 with PB2-627E or PB2-627K virus, which possesses glutamic acid or lysine at position 627 in the PB2 protein, respectively. Cells were incubated at 33°C or 37°C for the indicated time periods. Virus titers in MDCK cells were determined. The error bars represent standard deviations from three independent experiments. The statistical significance of the difference between the control and test samples is shown by P values, which were determined by Student's t test (**, $P < 0.01$; *, $P < 0.05$; black asterisks indicate the PB2-627K virus, and gray asterisks indicate the PB2-627E virus). (E) Influenza B virus and Sendai virus growth in shRSK2 cells. shRSK2 and control shGFP cells were infected at an MOI of 0.05 with influenza B virus or Sendai virus. At the indicated times after infection, cells were harvested and the virus titers in MDCK cells were determined. The error bars represent standard deviations from three independent experiments. The statistical significance of the difference between the control and test samples is shown by the P value, which was determined by Student's t test (**, $P < 0.01$; *, $P < 0.05$).

RSK family members are unusual among serine/threonine kinases in that they contain two distinct kinase domains that are sequentially activated (Fig. 1B). The C-terminal kinase domain (CKD) is activated by ERK1/2, which then triggers subsequent activation of the N-terminal kinase domain (NKD) (reviewed in reference 6). The NKD of RSK2 then phosphorylates a broad range of substrates, including cAMP response element-binding protein, c-Fos, glycogen synthase kinase 3, and many others (reviewed in reference 6). ΔN-RSK2 contains the entire CKD of this protein (Fig. 1B) and may sequester free ERK1/2, thereby preventing activation of functional RSK2. Thus, we speculated that full-length RSK2 has antiviral activity and that ΔN-RSK2 acts as a dominant-negative factor that suppresses RSK2 and its antiviral activity, resulting in increased viral replication.

To test our hypothesis that RSK2 has antiviral activity against influenza virus, we knocked down RSK2 in 293 (human embryonic kidney) cells using a retroviral vector expressing shRNA specific to human RSK2. RSK2 expression was reduced to approximately 15% in shRSK2 cells relative to the expression level in control shGFP cells, which express shRNA against GFP (Fig. 2A). As speculated, RSK2 knockdown resulted in increased viral polymerase activity for PB2-627E at 33°C (Fig. 2B) and, as a consequence, resulted in increased production of the viral M1 protein (Fig. 2C).

The data obtained thus far indicate that RSK2 suppresses influenza virus replication. However, the question of whether RSK2 interferes with influenza virus replication in general or in a strain- or host-specific manner remains unanswered. To address this question, we generated influenza viruses that possessed either a lysine at position 627 of PB2 (PB2-627K), which confers efficient replication in mammalian cells at 33°C and

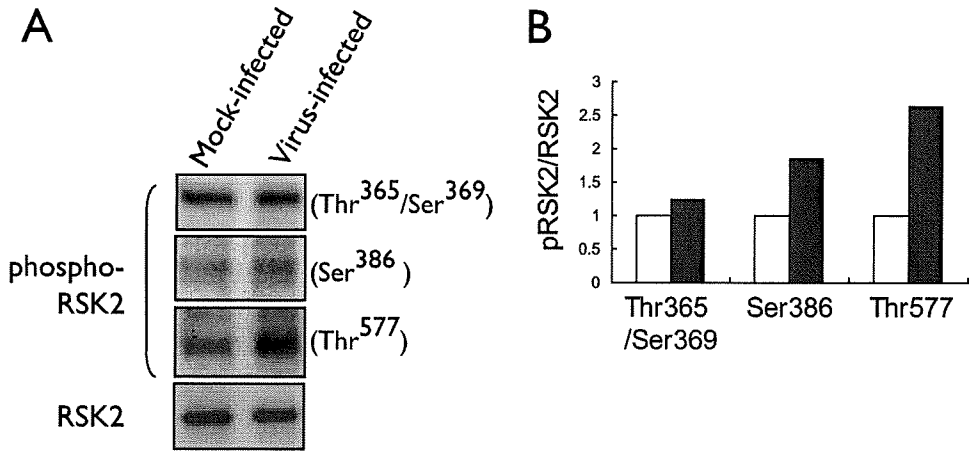

FIG. 3. Influenza virus-induced phosphorylation of RSK2. (A) 293 cells were infected with the PB2-627K virus (MOI of 3.0) or remained mock infected. Three or 5 hours later, cell lysates were immunoprecipitated with anti-RSK2 antibody, followed by Western blot analysis with the indicated antibodies to phosphorylated forms of RSK2. (B) Graphical representation of data shown in panel A. The relative ratios of phosphorylated to nonphosphorylated RSK2 are depicted. Influenza virus infection results in phosphorylation of RSK2. White bars, mock-infected cells; black bars, virus-infected cells.

37°C, or a glutamic acid at this position (PB2-627E), which results in attenuation of replication in mammalian cells at 33°C and, to a lesser extent, at 37°C. Growth of both viruses at 33°C and 37°C in shRSK2 cells and control shGFP cells was tested. Briefly, cells were infected at an MOI of 0.05 with PB2-627E or PB2-627K virus and virus titers in the culture supernatant were determined by plaque formation assays of MDCK cells at various times postinfection. As expected, the PB2-627K virus grew more efficiently than the PB2-627E virus in control shGFP cells at 33°C (Fig. 2D, left), while only minor differences in growth were observed for PB2-627K and PB2-627E viruses in control shGFP cells at 37°C (Fig. 2D, right); these findings are consistent with our earlier data (17). By comparing viral growth properties in control shGFP and shRSK2 cells, we found more-efficient growth in shRSK2 cells for both viruses at both temperatures, demonstrating that the nature of the amino acid at position 627 of PB2 does not affect the antiviral effect mediated by RSK2; all subsequent infection experiments were therefore carried out with the PB2-627K virus. Together, these findings indicate that RSK2 is a general antiviral host factor that suppresses influenza A virus replication.

To further examine the antiviral function of RSK2, we assessed the growth kinetics of an influenza B virus and Sendai virus (a negative-sense RNA virus belonging to the family *Paramyxoviridae*) in shRSK2 and shGFP control cells (Fig. 2E). These viruses grew more efficiently in shRSK2 cells than in control shGFP cells. Hence, RSK2 may have broad antiviral effects; for example, it may trigger an innate immune responses.

In quiescent cells, RSK2 is maintained in an inactive form in a complex with ERK1/2 (reviewed in reference 42). Interaction with phosphorylated ERK1/2 results in RSK2 phosphorylation, dissociation from ERK1/2, and (partial) translocation to the nucleus (7). To assess whether RSK2 is activated upon influenza virus infection, we immunoprecipitated RSK2 from cell lysates obtained from influenza virus- or mock-infected cells and subsequently evaluated the phosphorylation status of RSK2 using antibodies specific to distinct phosphorylated forms of RSK2. Influenza virus infection resulted in increased levels of phosphorylated RSK2 compared to those in mock-infected cells (Fig. 3A and B). The most efficient induction of phosphorylation was observed for Thr577. This residue is phosphorylated by ERK1/2, resulting in the activation of RSK2 and the subsequent autophosphorylation of other phosphorylation sites, such as Ser386 (reviewed in reference 6). The observed phosphorylation of RSK2 upon influenza infection may result from direct interaction with a viral component or from ERK1/2 signaling, as the "classical" MAPK (Raf/MEK/ERK) pathway is known to be activated by influenza virus infection (38).

Next, we assessed the mechanism(s) by which RSK2 affects influenza virus replication. RSK2 activates NF-κB (13, 43), a major player in innate immune responses to viral infections (reviewed in reference 19). Moreover, NF-κB is known to be activated upon influenza virus infection (35). Therefore, we speculated that influenza virus-induced activation of RSK2 may lead to the stimulation of NF-κB and subsequent induction of an antiviral response. To test this assumption, we expressed the luciferase reporter protein under the control of an NF-κB-dependent promoter in virus- or mock-infected shRSK2 and control shGFP cells (Fig. 2A). As expected, influenza A virus infection induced NF-κB promoter activity in shGFP cells (Fig. 4A); the level of promoter stimulation was similar to that published elsewhere (52). In contrast, no significant increase in NF-κB-dependent promoter activity was observed in virus-infected shRSK2 cells (Fig. 4A), suggesting that virus-induced NF-κB stimulation relies on RSK2 activation. This lack of activation was partially restored following transfection of shRSK2 cells with pmRSK2, which encodes a human RSK2 cDNA containing a silent mutation within the small interfering RNA target sequence (Fig. 4A). In conclusion, these findings suggest that RSK2 may affect influenza virus replication, at least in part, through NF-κB.

NF-κB stimulation leads to the expression of multiple cellular factors, including IFN-β, a central player in the innate immune response that is activated upon virus infection. We asked whether RSK2 activates IFN-β-stimulated promoters.

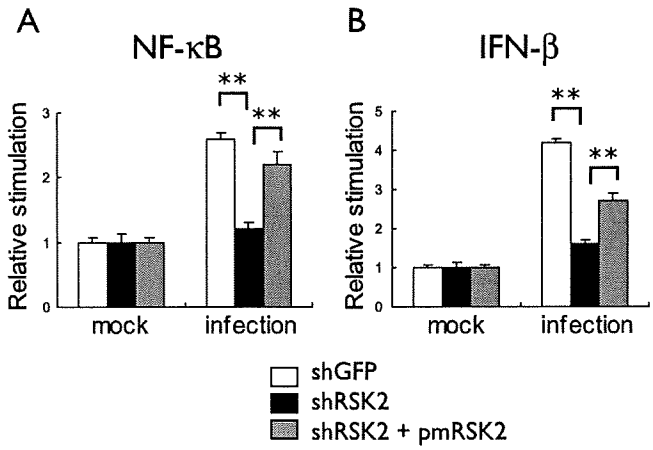

FIG. 4. Effect of RSK2 knockdown on influenza virus-induced activation of NF-κB- and IFN-β-dependent promoters. Plasmids that express luciferase under the control of NF-κB (A)- or IFN-β-dependent (B) promoters were transfected into shRSK2 or control shGFP cells. Nine hours posttransfection, cells were infected with the PB2-627K virus at an MOI of 1; control cells remained mock infected. After 12 hours of incubation at 33°C, cell lysates were prepared and subjected to luciferase assays. In a parallel experiment, cells were also transfected with pmRSK2, which encodes a silently mutagenized human RSK2 that is not recognized by the RSK2 shRNA. Influenza virus induced stimulation of NF-κB- and IFN-β-dependent promoters in shGFP cells (white bars); this stimulation is blocked by RSK2 knockdown (black bars) but can be partially restored upon expression of RSK2 that is insensitive to the RSK2 shRNA (gray bars). The error bars represent standard deviations from three independent experiments. P values were determined by Student's t test (**, $P < 0.01$).

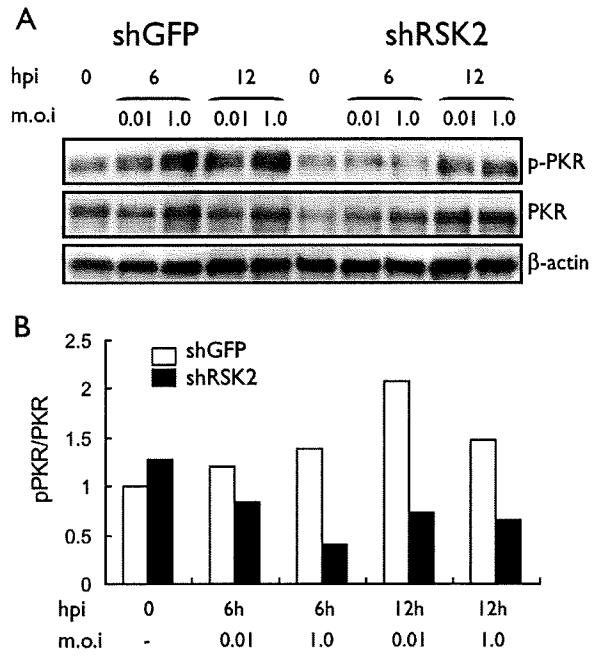

FIG. 5. Effect of RSK2 knockdown on influenza virus-induced phosphorylation of PKR. (A) shRSK2 cells and control shGFP cells were infected with the PB2-627K virus at an MOI of 0.01 or 1 and incubated at 33°C. At the indicated times postinfection, cell lysates were prepared and subjected to Western blot analysis with antibodies against PKR, phosphorylated PKR, or β-actin, which served as an internal control. hpi, hours postinfection. (B) Graphical representation of data shown in panel A. The relative ratios of phosphorylated to nonphosphorylated PKR are depicted. Influenza virus infection results in increased levels of phosphorylated PKR in control shGFP cells but not in shRSK2 cells.

We carried out experiments essentially as described in the previous section. That is, we cloned the luciferase gene under the control of an IFN-β-stimulated promoter and assayed luciferase expression in virus- and mock-infected shRSK2 and control shGFP cells (Fig. 4B). Influenza virus infection activated IFN-β-stimulated promoter activity in control shGFP cells (Fig. 4B) but not in shRSK2 cells (Fig. 4B). This impediment was partially overcome by transfection of shRSK2 cells with pmRSK2 (Fig. 4B). These results demonstrate that RSK2 activates both NF-κB and IFN-β signaling pathways upon influenza infection in 293 cells.

PKR is an important component of IFN-mediated antiviral responses (reviewed in reference 15). This kinase phosphorylates the α subunit of eukaryotic initiation factor 2, resulting in rapid inhibition of translation and restriction of the spread of the virus (2, 3, 11, 14). Recently, PKR was also identified as an RSK2 substrate (53). We tested whether RSK2 affects influenza virus replication through PKR phosphorylation and activation. As expected, phosphorylation of PKR upon influenza virus infection was apparent in control shGFP cells (Fig. 5A; Fig. 5B shows an increasing ratio of phosphorylated to nonphosphorylated PKR upon virus infection). In contrast, PKR phosphorylation was suppressed in shRSK2 cells (Fig. 5A and B), indicating that influenza virus-induced activation of RSK2 results in PKR phosphorylation in 293 cells.

In summary, we demonstrated that the MAPK-activated protein kinase RSK2 plays a role in the innate immune response to influenza virus infection, as shown in Fig. 6. RSK2 is known to phosphorylate cellular factors involved in cell proliferation, regulation of transcription, regulation of translation, cell survival, and apoptosis (reviewed in reference 6) and may affect viral growth through these processes. The human immunodeficiency virus Tat protein is known to interact with RSK2 (18), resulting in RSK2 activation. Activated RSK2 is, in turn,

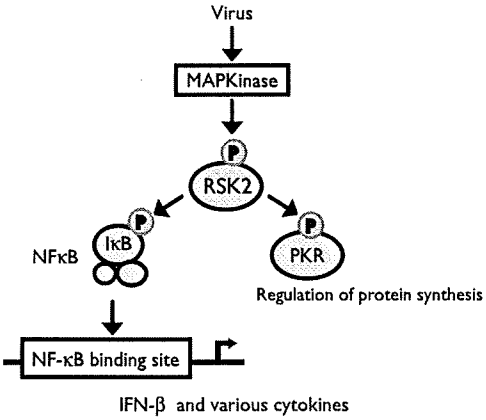

FIG. 6. Putative role of RSK2 in antiviral signaling. Influenza virus infection may activate RSK2 through MAPK kinase signaling pathways or through direct interaction with a viral component. Our data suggest that RSK2 activation is needed for efficient stimulation of NF-κB, IFN-β, and PKR, all of which play major roles in the cellular antiviral response.

critical for the transcriptional activity of Tat (18). Another study demonstrated that ORF45 of the Kaposi's sarcoma-associated herpesvirus interacts with RSK1 and RSK2, resulting in their stimulation (22). Further studies suggest that RSK1/2 upregulation plays a critical role in the lytic replication of Kaposi's sarcoma-associated herpesvirus (22). Another study suggested that RSK2 signaling is important for efficient vaccinia virus amplification (1). It is interesting to note that these studies ascribe a virus-supportive role to RSK2 activation.

In contrast to the above-mentioned studies, which found a virus-supportive role for RSK2, our findings suggest an antiviral activity for this kinase. In particular, we found that the C-terminal domain of RSK2, which acts in a dominant-negative manner, and a small interfering RNA to RSK2 increased influenza virus polymerase activity in in vitro assays and/or enhanced influenza virus replication. RSK2 is known to be activated by the Raf/MEK/ERK signaling cascade (reviewed in reference 24). Studies by Pleschka et al. (39) suggest that this pathway has a virus-supportive function. This finding seems to contradict our finding that RSK2 has antiviral activity. However, the virus-supportive function of the Raf/MEK/ERK signaling cascade was established by use of an inhibitor to MEK (39), which may affect several pathways that are controlled by MEK/ERK. In addition, activation of RSK1/2 is controlled not only by ERK1/2, but also by other MAPKs, such as p38 (reviewed in references 10 and 40), which is activated upon influenza virus infection and triggers an antiviral response (8). Collectively, the current data suggest that RSK2 is activated by both virus-supportive and -antagonistic signaling pathways and that the complex interplay of these factors and pathways determines its downstream effects.

Our data suggest that RSK2 may execute its antiviral function through NF-κB. Some studies have found a supportive role for NF-κB in influenza virus infection (32, 50), while another study suggested that NF-κB activation is not required for efficient influenza virus replication (5). In general, the role of NF-κB in the regulation of IFN-β responses is still not well understood. Recent studies found that NF-κB stimulates the expression of certain IFN-stimulated genes, while it suppresses others (37). As discussed earlier, viral infections trigger multiple cellular pathways that stimulate both agonistic and antagonistic functions; the outcome of a viral infection may ultimately be determined by the complex and as yet poorly understood interplay between these virus-supportive and -antagonistic factors.

We found that RSK2 affects influenza virus replication through innate immune response pathways (Fig. 6). Although RSK2 is known to activate NF-κB (13, 43) and PKR (53), it had not been recognized as a critical signaling component in innate immune responses to viral infections. We found, however, that RSK2 knockdown in 293 cells affected the influenza virus-induced activation of NF-κB and IFN-β and the influenza virus-induced phosphorylation of PKR, suggesting a critical role for RSK2 in innate immune responses to viral infections. In fact, we found that RSK2 knockdown not only increased influenza A virus titers but also stimulated influenza B virus and Sendai virus replication. In conclusion, we have identified a role for RSK2 in innate immune responses to influenza A virus infection, which may be executed through the regulation of IFN-β, NF-κB, and PKR responses. Other MAPK-activated protein kinases may have similar, as of yet unidentified, functions in the innate immune response and antiviral defense mechanisms.

ACKNOWLEDGMENTS

We thank Susan Watson for editing the manuscript and Hideo Iba for providing us with plasmids for the retroviral vector-mediated RNA interference studies.

This research was supported by grants-in-aid from the Ministry of Education, Culture, Sports, Science, and Technology of Japan, by ERATO (Japan Science and Technology Agency), and by National Institute of Allergy and Infectious Diseases Public Health Service research grants.

REFERENCES

1. **Andrade, A. A., P. N. Silva, A. C. Pereira, L. P. De Sousa, P. C. Ferreira, R. T. Gazzinelli, E. G. Kroon, C. Ropert, and C. A. Bonjardim.** 2004. The vaccinia virus-stimulated mitogen-activated protein kinase (MAPK) pathway is required for virus multiplication. Biochem. J. **381**:437–446.
2. **Balachandran, S., P. C. Roberts, L. E. Brown, H. Truong, A. K. Pattnaik, D. R. Archer, and G. N. Barber.** 2000. Essential role for the dsRNA-dependent protein kinase PKR in innate immunity to viral infection. Immunity **13**:129–141.
3. **Barber, G. N.** 2005. The dsRNA-dependent protein kinase, PKR and cell death. Cell Death Differ. **12**:563–570.
4. **Bergmann, M., A. Garcia-Sastre, E. Carnero, H. Pehamberger, K. Wolff, P. Palese, and T. Muster.** 2000. Influenza virus NS1 protein counteracts PKR-mediated inhibition of replication. J. Virol. **74**:6203–6206.
5. **Bernasconi, D., C. Amici, S. La Frazia, A. Ianaro, and M. G. Santoro.** 2005. The IkappaB kinase is a key factor in triggering influenza A virus-induced inflammatory cytokine production in airway epithelial cells. J. Biol. Chem. **280**:24127–24134.
6. **Carriere, A., H. Ray, J. Blenis, and P. P. Roux.** 2008. The RSK factors of activating the Ras/MAPK signaling cascade. Front. Biosci. **13**:4258–4275.
7. **Chen, R. H., C. Sarnecki, and J. Blenis.** 1992. Nuclear localization and regulation of *erk*- and *rsk*-encoded protein kinases. Mol. Cell. Biol. **12**:915–927.
8. **Conze, D., J. Lumsden, H. Enslen, R. J. Davis, G. Le Gros, and M. Rincón.** 2000. Activation of p38 MAP kinase in T cells facilitates the immune response to the influenza virus. Mol. Immunol. **37**:503–513.
9. **Donelan, N. R., C. F. Basler, and A. García-Sastre.** 2003. A recombinant influenza A virus expressing an RNA-binding-defective NS1 protein induces high levels of beta interferon and is attenuated in mice. J. Virol. **77**:13257–13266.
10. **Gaestel, M.** 2008. Specificity of signaling from MAPKs to MAPKAPKs: kinases' tango nuevo. Front. Biosci. **13**:6050–6059.
11. **Gale, M., Jr., and M. G. Katze.** 1998. Molecular mechanisms of interferon resistance mediated by viral-directed inhibition of PKR, the interferon-induced protein kinase. Pharmacol. Ther. **78**:29–46.
12. **Geiss, G. K., M. Salvatore, T. M. Tumpey, V. S. Carter, X. Wang, C. F. Basler, J. K. Taubenberger, R. E. Bumgarner, P. Palese, M. G. Katze, and A. García-Sastre.** 2002. Cellular transcriptional profiling in influenza A virus-infected lung epithelial cells: the role of the nonstructural NS1 protein in the evasion of the host innate defense and its potential contribution to pandemic influenza. Proc. Natl. Acad. Sci. USA **99**:10736–10741.
13. **Ghoda, L., X. Lin, and W. C. Greene.** 1997. The 90-kDa ribosomal S6 kinase (pp90rsk) phosphorylates the N-terminal regulatory domain of IkappaBalpha and stimulates its degradation in vitro. J. Biol. Chem. **272**:21281–21288.
14. **Goodman, A. G., J. A. Smith, S. Balachandran, O. Perwitasari, S. C. Proll, M. J. Thomas, M. J. Korth, G. N. Barber, L. A. Schiff, and M. G. Katze.** 2007. The cellular protein P58IPK regulates influenza virus mRNA translation and replication through a PKR-mediated mechanism. J. Virol. **81**:2221–2223.
15. **Haller, O., G. Kochs, and F. Weber.** 2007. Interferon, Mx, and viral countermeasures. Cytokine Growth Factor Rev. **18**:425–433.
16. **Hatta, M., P. Gao, P. Halfmann, and Y. Kawaoka.** 2001. Molecular basis for high virulence of Hong Kong H5N1 influenza A viruses. Science **293**:1840–1842.
17. **Hatta, M., Y. Hatta, J. H. Kim, S. Watanabe, K. Shinya, T. Nguyen, P. S. Lien, Q. M. Le, and Y. Kawaoka.** 2007. Growth of H5N1 influenza A viruses in the upper respiratory tracts of mice. PLoS Pathog. **3**:1374–1379.
18. **Hetzer, C., D. Bisgrove, M. S. Cohen, A. Pedal, K. Kaehlcke, A. Speyerer, K. Bartscherer, J. Taunton, and M. Ott.** 2007. Recruitment and activation of RSK2 by HIV-1 Tat. PLoS ONE **2**:e151.
19. **Hiscott, J., H. Kwon, and P. Génin.** 2001. Hostile takeovers: viral appropriation of the NF-kappaB pathway. J. Clin. Investig. **107**:143–151.
20. **Kitamura, T., and Y. Morikawa.** 2000. Isolation of T-cell antigens by retrovirus-mediated expression cloning. Methods Mol. Biol. **134**:143–152.
21. **Kochs, G., A. García-Sastre, and L. Martínez-Sobrido.** 2007. Multiple anti-

interferon actions of the influenza A virus NS1 protein. J. Virol. **81**:7011–7021.
22. **Kuang, E., Q. Tang, G. G. Maul, and F. Zhu.** 2008. Activation of p90 ribosomal S6 kinase by ORF45 of Kaposi's sarcoma-associated herpesvirus and its role in viral lytic replication J. Virol. **82**:1838–1850.
23. **Kujime, K., S. Hashimoto, Y. Gon, K. Shimizu, and T. Horie.** 2000. p38 mitogen-activated protein kinase and c-jun-NH2-terminal kinase regulate RANTES production by influenza virus-infected human bronchial epithelial cells. J. Immunol. **164**:3222–3228.
24. **Lu, Z., and S. Xu.** 2006. ERK1/2 MAP kinases in cell survival and apoptosis. IUBMB Life **58**:621–631.
25. **Ludwig, S., C. Ehrhardt, E. R. Neumeier, M. Kracht, U. R. Rapp, and S. Pleschka.** 2001. Influenza virus-induced AP-1-dependent gene expression requires activation of the JNK signaling pathway. J. Biol. Chem. **276**:10990–10998.
26. **Ludwig, S., O. Planz, S. Pleschka, and T. Wolff.** 2003. Influenza-virus-induced signaling cascades: targets for antiviral therapy? Trends Mol. Med. **9**:46–52.
27. **Ludwig, S., S. Pleschka, O. Planz, and T. Wolff.** 2006. Ringing the alarm bells: signalling and apoptosis in influenza virus infected cells. Cell. Microbiol. **8**:375–386.
28. **Massin, P., S. van der Werf, and N. Naffakh.** 2001. Residue 627 of PB2 is a determinant of cold sensitivity in RNA replication of avian influenza viruses. J. Virol. **75**:5398–5404.
29. **Mibayashi, M., L. Martínez-Sobrido, Y. M. Loo, W. B. Cárdenas, M. Gale, Jr., and A. García-Sastre.** 2007. Inhibition of retinoic acid-inducible gene I-mediated induction of beta interferon by the NS1 protein of influenza A virus. J. Virol. **81**:514–524.
30. **Min, J. Y., and R. M. Krug.** 2006. The primary function of RNA binding by the influenza A virus NS1 protein in infected cells: inhibiting the 2′-5′ oligo(A) synthetase/RNase L pathway. Proc. Natl. Acad. Sci. USA **103**:7100–7105.
31. **Neumann, G., T. Watanabe, H. Ito, S. Watanabe, H. Goto, P. Gao, M. Hughes, D. R. Perez, R. Donis, E. Hoffmann, G. Hobom, and Y. Kawaoka.** 1999. Generation of influenza A viruses entirely from cloned cDNAs. Proc. Natl. Acad. Sci. USA **96**:9345–9350.
32. **Nimmerjahn, F., D. Dudziak, U. Dirmeier, G. Hobom, A. Riedel, M. Schlee, L. M. Staudt, A. Rosenwald, U. Behrends, G. W. Bornkamm, and J. Mautner.** 2004. Active NF-kappaB signalling is a prerequisite for influenza virus infection. J. Gen. Virol. **85**:2347–2356.
33. **Niwa, H., K. Yamamura, and J. Miyazaki.** 1991. Efficient selection for high-expression transfectants with a novel eukaryotic vector. Gene **108**:193–199.
34. **Onishi, M., S. Kinoshita, Y. Morikawa, A. Shibuya, J. Phillips, L. L. Lanier, D. M. Gorman, G. P. Nolan, A. Miyajima, and T. Kitamura.** 1996. Applications of retrovirus-mediated expression cloning. Exp. Hematol. **24**:324–329.
35. **Pahl, H. L., and P. A. Baeuerle.** 1995. Expression of influenza virus hemagglutinin activates transcription factor NF-κB. J. Virol. **69**:1480–1484.
36. **Palese, P.** 2007. Orthomyxoviridae, p. 1649–1689. *In* D. M. Knipe, P. M. Howley, D. E. Griffin, R. A. Lamb, M. A. Martin, B. Roizman, and S. E. Straus (ed.), Fields virology, 5th ed. Lippincott Williams & Wilkins, Philadelphia, PA.
37. **Pfeffer, L. M., J. G. Kim, S. R. Pfeffer, D. J. Carrigan, D. P. Baker, L. Wei, and R. Homayouni.** 2004. Role of nuclear factor-kappaB in the antiviral action of interferon and interferon-regulated gene expression. J. Biol. Chem. **279**:31304–31311.
38. **Pleschka, S.** 2008. RNA viruses and the mitogenic Raf/MEK/ERK signal transduction cascade. Biol. Chem. [Epub ahead of print] doi:10.1515/BC.2008.145.
39. **Pleschka, S., T. Wolff, C. Ehrhardt, G. Hobom, O. Planz, U. R. Rapp, and S. Ludwig.** 2001. Influenza virus propagation is impaired by inhibition of the Raf/MEK/ERK signalling cascade. Nat. Cell Biol. **3**:301–305.
40. **Raman, M., W. Chen, and M. H. Cobb.** 2007. Differential regulation and properties of MAPKs. Oncogene **26**:3100–3112.
41. **Roux, P. P., and J. Blenis.** 2004. ERK and p38 MAPK-activated protein kinases: a family of protein kinases with diverse biological functions. Microbiol. Mol. Biol. Rev. **68**:320–344.
42. **Roux, P. P., S. A. Richards, and J. Blenis.** 2003. Phosphorylation of p90 ribosomal S6 kinase (RSK) regulates extracellular signal-regulated kinase docking and RSK activity. Mol. Cell. Biol. **23**:4796–4804.
43. **Schouten, G. J., A. C. Vertegaal, S. T. Whiteside, A. Israël, M. Toebes, J. C. Dorsman, A. J. van der Eb, and A. Zantema.** 1997. IkappaB alpha is a target for the mitogen-activated 90 kDa ribosomal S6 kinase. EMBO J. **16**:3133–3144.
44. **Shimojima, M., T. Miyazawa, Y. Ikeda, E. L. McMonagle, H. Haining, H. Akashi, Y. Takeuchi, M. J. Hosie, and B. J. Willett.** 2004. Use of CD134 as a primary receptor by the feline immunodeficiency virus. Science **303**:1192–1195.
45. **Shimojima, M., T. Miyazawa, Y. Sakurai, Y. Nishimura, Y. Tohya, Y. Matsuura, and H. Akashi.** 2003. Usage of myeloma and panning in retrovirus-mediated expression cloning. Anal. Biochem. **315**:138–140.
46. **Shinya, K., S. Hamm, M. Hatta, H. Ito, T. Ito, and Y. Kawaoka.** 2004. PB2 amino acid at position 627 affects replicative efficiency, but not cell tropism, of Hong Kong H5N1 influenza A viruses in mice. Virology **320**:258–266.
47. **Subbarao, E. K., W. London, and B. R. Murphy.** 1993. A single amino acid in the PB2 gene of influenza A virus is a determinant of host range. J. Virol. **67**:1761–1764.
48. **Talon, J., C. M. Horvath, R. Polley, C. F. Basler, T. Muster, P. Palese, and A. García-Sastre.** 2000. Activation of interferon regulatory factor 3 is inhibited by the influenza A virus NS1 protein. J. Virol. **74**:7989–7996.
49. **Wang, X., M. Li, H. Zheng, T. Muster, P. Palese, A. A. Beg, and A. García-Sastre.** 2000. Influenza A virus NS1 protein prevents activation of NF-κB and induction of alpha/beta interferon. J. Virol. **74**:11566–11573.
50. **Wei, L., M. R. Sandbulte, P. G. Thomas, R. J. Webby, R. Homayouni, and L. M. Pfeffer.** 2006. NFkappaB negatively regulates interferon-induced gene expression and anti-influenza activity. J. Biol. Chem. **281**:11678–11684.
51. **Wright, P. F.** 2007. Orthomyxoviruses, p. 1691–1740. *In* D. M. Knipe, P. M. Howley, D. E. Griffin, R. A. Lamb, M. A. Martin, B. Roizman, and S. E. Straus (ed.), Fields virology, 5th ed. Lippincott Williams & Wilkins, Philadelphia, PA.
52. **Wurzer, W. J., C. Ehrhardt, S. Pleschka, F. Berberich-Siebelt, T. Wolff, H. Walczak, O. Planz, and S. Ludwig.** 2004. NF-kappaB-dependent induction of tumor necrosis factor-related apoptosis-inducing ligand (TRAIL) and Fas/FasL is crucial for efficient influenza virus propagation. J. Biol. Chem. **279**:30931–30937.
53. **Zykova, T. A., F. Zhu, Y. Zhang, A. M. Bode, and Z. Dong.** 2007. Involvement of ERKs, RSK2 and PKR in UVA-induced signal transduction toward phosphorylation of eIF2alpha (Ser(51)). Carcinogenesis **28**:1543–1551.

LETTERS

In vitro and *in vivo* characterization of new swine-origin H1N1 influenza viruses

Yasushi Itoh[1], Kyoko Shinya[2], Maki Kiso[3], Tokiko Watanabe[4], Yoshihiro Sakoda[5], Masato Hatta[4], Yukiko Muramoto[6], Daisuke Tamura[3], Yuko Sakai-Tagawa[3], Takeshi Noda[7], Saori Sakabe[3], Masaki Imai[4], Yasuko Hatta[4], Shinji Watanabe[4], Chengjun Li[4], Shinya Yamada[3], Ken Fujii[6], Shin Murakami[3], Hirotaka Imai[3], Satoshi Kakugawa[3], Mutsumi Ito[3], Ryo Takano[3], Kiyoko Iwatsuki-Horimoto[3], Masayuki Shimojima[3], Taisuke Horimoto[3], Hideo Goto[3], Kei Takahashi[3], Akiko Makino[2], Hirohito Ishigaki[1], Misako Nakayama[1], Masatoshi Okamatsu[5], Kazuo Takahashi[8], David Warshauer[9], Peter A. Shult[9], Reiko Saito[10], Hiroshi Suzuki[10], Yousuke Furuta[11], Makoto Yamashita[12], Keiko Mitamura[13], Kunio Nakano[13], Morio Nakamura[13], Rebecca Brockman-Schneider[14], Hiroshi Mitamura[15], Masahiko Yamazaki[16], Norio Sugaya[17], M. Suresh[4], Makoto Ozawa[4,7], Gabriele Neumann[4], James Gern[14], Hiroshi Kida[5], Kazumasa Ogasawara[1] & Yoshihiro Kawaoka[2,3,4,6,7,18]

Influenza A viruses cause recurrent outbreaks at local or global scale with potentially severe consequences for human health and the global economy. Recently, a new strain of influenza A virus was detected that causes disease in and transmits among humans, probably owing to little or no pre-existing immunity to the new strain. On 11 June 2009 the World Health Organization declared that the infections caused by the new strain had reached pandemic proportion. Characterized as an influenza A virus of the H1N1 subtype, the genomic segments of the new strain were most closely related to swine viruses[1]. Most human infections with swine-origin H1N1 influenza viruses (S-OIVs) seem to be mild; however, a substantial number of hospitalized individuals do not have underlying health issues, attesting to the pathogenic potential of S-OIVs. To achieve a better assessment of the risk posed by the new virus, we characterized one of the first US S-OIV isolates, A/California/04/09 (H1N1; hereafter referred to as CA04), as well as several other S-OIV isolates, *in vitro* and *in vivo*. In mice and ferrets, CA04 and other S-OIV isolates tested replicate more efficiently than a currently circulating human H1N1 virus. In addition, CA04 replicates efficiently in non-human primates, causes more severe pathological lesions in the lungs of infected mice, ferrets and non-human primates than a currently circulating human H1N1 virus, and transmits among ferrets. In specific-pathogen-free miniature pigs, CA04 replicates without clinical symptoms. The assessment of human sera from different age groups suggests that infection with human H1N1 viruses antigenically closely related to viruses circulating in 1918 confers neutralizing antibody activity to CA04. Finally, we show that CA04 is sensitive to approved and experimental antiviral drugs, suggesting that these compounds could function as a first line of defence against the recently declared S-OIV pandemic.

Sequence analyses of recently emerged swine-origin H1N1 viruses (S-OIVs) revealed the absence of markers associated with high pathogenicity in avian and/or mammalian species, such as a multibasic haemagglutinin (HA) cleavage site[2] or lysine at position 627 of the PB2 protein[3]. To characterize the new viruses *in vitro* and *in vivo*, we amplified the following S-OIVs in Madin–Darby canine kidney (MDCK) cells: A/California/04/09 (CA04), A/Wisconsin/WSLH049/09 (WSLH049), A/Wisconsin/WSLH34939/09 (WSLH34939), A/Netherlands/603/09 (Net603) and A/Osaka/164/09 (Osaka164). WSLH34939 was isolated from a patient who required hospitalization, whereas the remaining viruses were isolated from mild cases. These viruses represent the currently recognized neuraminidase (NA) variants among S-OIVs: CA04, NA-106V, NA-248N; Osaka164, NA-106I, NA-248N; WSLH049, NA-106I, NA-248D; WSLH34939, NA-106I, NA-248D; and Net603, NA-106V, NA-248N.

In MDCK cells and primary human airway epithelial cells, CA04 grew to titres comparable to those typically obtained for contemporary human H1N1 influenza viruses (Supplementary Fig. 1). Confocal, transmission electron and scanning electron microscopy revealed virions of remarkably filamentous shape (Supplementary Fig. 2), in marked contrast to the spherical shape observed with negatively stained virions (http://www.cdc.gov/h1n1flu/images.htm). The biological significance of the morphology of CA04 remains unknown.

To evaluate the pathogenicity of S-OIV in mammalian models, we conducted studies in mice, ferrets, non-human primates and pigs. BALB/c mice intranasally infected with a high dose ($>10^4$ plaque-forming units (p.f.u.)) of CA04 (Supplementary Fig. 3) experienced weight loss and those infected with the highest dose of this virus were humanely killed, in contrast to animals infected with a recent human H1N1 virus (A/Kawasaki/UTK-4/09, KUTK-4). The 50% mouse lethal dose (MLD_{50}) was $10^{5.8}$ p.f.u. for CA04 and $>10^{6.6}$ p.f.u. for

[1]Department of Pathology, Shiga University of Medical Science, Ohtsu, Shiga 520-2192, Japan. [2]Department of Microbiology and Infectious Diseases, Kobe University, Hyogo 650-0017, Japan. [3]Division of Virology, Department of Microbiology and Immunology, Institute of Medical Science, University of Tokyo, Tokyo 108-8639, Japan. [4]Department of Pathobiological Sciences, University of Wisconsin-Madison, Madison, Wisconsin 53711, USA. [5]Department of Disease Control, Graduate School of Veterinary Medicine, Hokkaido University, Sapporo 060-0818, Japan. [6]ERATO Infection-Induced Host Responses Project, Saitama 332-0012, Japan. [7]Department of Special Pathogens, International Research Center for Infectious Diseases, Institute of Medical Science, University of Tokyo, Tokyo 108-8639, Japan. [8]Department of Infectious Diseases, Osaka Prefectural Institute of Public Health, Osaka 537-0025, Japan. [9]Wisconsin State Laboratory of Hygiene, Madison, Wisconsin 53706, USA. [10]Department of Public Health, Niigata University, Graduate School of Medical and Dental Sciences, Niigata 951-8510, Japan. [11]Toyama Chemical Co., Ltd., Toyama 930-8508, Japan. [12]Daiichi Sankyo Co Ltd, Shinagawa, Tokyo 140-8710, Japan. [13]Eiju General Hospital, Tokyo 110-8654, Japan. [14]School of Medicine and Public Health, University of Wisconsin-Madison, Madison, Wisconsin 53792, USA. [15]Department of Internal Medicine, Mitamura Clinic, Shizuoka 413-0103, Japan. [16]Department of Pediatrics, Zama Children's Clinic, Kanagawa 228-0023, Japan. [17]Keiyu Hospital, Kanagawa 220-0012, Japan. [18]Creative Research Initiative, Sousei, Hokkaido University, Sapporo 060-0818, Japan.

KUTK-4. For the additional S-OIV isolates tested, the MLD_{50} values were $>10^{6.4}$ p.f.u. for Osaka164, $>10^{6.6}$ p.f.u. for WSLH049, $10^{4.5}$ p.f.u. for WSLH34939 and $>10^{5.8}$ p.f.u. for Net603.

On day 3 after infection of mice, similar titres were detected in nasal turbinates of mice infected with 10^5 p.f.u. of S-OIVs or KUTK-4 (Supplementary Table 1); however, S-OIVs replicated more efficiently in the lungs of infected animals, which may account for the prominent bronchitis and alveolitis with viral antigen on day 3 after infection with CA04 (Supplementary Fig. 4a, b). On day 6 after infection, virus titres followed a similar trend and the lungs of CA04-infected mice showed bronchitis and alveolitis with viral antigen, although signs of regeneration were apparent (Supplementary Fig. 4c). We detected viral-antigen-positive bronchial epithelial cells, but not alveolar cells, on day 3 after infection of mice infected with KUTK-4 (Supplementary Fig. 4e). By day 6, infection in KUTK-4-inoculated mice had progressed to bronchitis and peribronchitis; however, viral antigen was rarely detected in these lesions (Supplementary Fig. 4f).

There were marked differences in the induction of pro-inflammatory cytokines in the lungs of mice infected with CA04 compared with KUTK-4 (Supplementary Fig. 5a–c). Infection with KUTK-4 resulted in limited induction of pro-inflammatory cytokines/chemokines in the lungs, in marked contrast to infection with CA04. Increased production of interleukin-10 (IL-10; Supplementary Fig. 5a) in lungs of CA04-infected mice at day 6 after infection probably reflects a host response to dampen over-exuberant pulmonary inflammation and promote tissue repair. Infection with CA04 led to strong induction of both interferon-γ (IFN-γ) and IL-4 in the lungs. The selective induction of the T_H2 cytokine IL-5 in CA04-infected, but not in KUTK-4-infected, mice on day 6 after infection is noteworthy (Supplementary Fig. 5b), but further studies are needed to understand the relevance of this finding to viral control. IL-17 has been reported to have a role in protection against lethal influenza and also in eliciting inflammatory responses[4,5]; however, the enhanced viral replication and lung pathology observed in CA04-infected mice was not linked to dysregulated IL-17 production.

Cynomolgus macaques (*Macaca fascicularis*) have been used to study highly pathogenic avian H5N1 viruses[6,7] and the 1918 pandemic virus[8]. Infection of cynomolgus macaques with CA04 (see Methods for detailed procedures) resulted in a more prominent increase in body temperature than infection with KUTK-4 (Supplementary Fig. 6). This difference might originate from the observed differences in virus titres (Table 1 and Supplementary Table 2). No remarkable difference in body weight loss was found between the two groups (data not shown). CA04 replicated efficiently in the lungs and other respiratory organs of infected animals, similar to highly pathogenic influenza viruses[6,8] (Table 1). By contrast, conventional human influenza viruses are typically limited in their replicative ability in the lungs of infected primates[6,8] (Table 1), although a seasonal H1N1 virus was isolated from one animal on day 7 after infection. Pathological examination revealed that CA04 caused more severe lung lesions than did KUTK-4 (Fig. 1 and Supplementary Fig. 7). On day 3 after infection with CA04, alveolar spaces were occupied by oedematous exudate and inflammatory infiltrates (Fig. 1a, b); severe thickening of alveolar walls was also observed (Fig. 1b). Viral-antigen-positive cells were distributed in the inflammatory lesions, and many of these cells were elongated with thin cytoplasm and hemming around the alveolar wall, indicating type I pneumocytes (Fig. 1c). In addition to type I pneumocytes, CA04 viral antigens were also detected in considerable numbers of cuboidal, cytokeratin-positive cells, hence identified as type II pneumocytes (Fig. 1d and Supplementary Fig. 8), as has been reported for highly pathogenic avian H5N1 influenza viruses[6]. Upon infection with KUTK-4, large sections of infected lungs showed thickening of the alveolar wall on day 3 after infection (Fig. 1e). Although the infiltration of inflammatory cells was prominent at the alveolar wall (Fig. 1f), viral antigens were sparse and detected in type I (but not type II) pneumocytes (Fig. 1g). By contrast, the lungs of non-infected animals show clear alveolar spaces (Fig. 1h).

On day 7 after infection, lung pathology remained more severe for CA04- than for KUTK-4-infected lungs (Supplementary Fig. 7), although regenerative changes were seen for CA04. Nonetheless, considerable numbers of antigen-positive cells were still detectable (Supplementary Fig. 7c). Collectively, these findings demonstrate that CA04 causes more severe lung lesions in non-human primates than does a contemporary human influenza virus.

Induction of pro-inflammatory cytokines/chemokines in the lungs of CA04-infected macaques was variable at day 3 after infection (Supplementary Fig. 9). However, consistent with persisting lung pathology and inflammation on day 7 after infection, the levels of MCP-1, MIP-1α, IL-6 and IL-18 were markedly higher in the lungs of two of three CA04-infected macaques.

Ferrets are widely accepted as a suitable small-animal model for influenza virus pathogenicity and transmissibility studies. Infection of ferrets with S-OIVs or KUTK-4 did not cause marked changes in body temperature or weight in any group (data not shown). Although all test viruses were detected in nasal turbinates at similar titres on day 3 after infection (Supplementary Table 3), S-OIVs replicated to higher titres in trachea and lungs.

Pathological examination detected similar levels of viral antigen in the nasal mucosa of both CA04- and KUTK-4-infected ferrets (Supplementary Fig. 10a and e). However, the lungs of CA04-infected ferrets showed more severe bronchopneumonia with prominent viral antigen expression in the peribronchial glands and a few alveolar cells (Supplementary Fig. 10b–d) on day 3 after infection. By contrast, most of the lung appeared normal after infection with

Table 1 | Virus titres in organs of infected cynomolgus macaques

Organ	A/California/04/09 (H1N1)						A/Kawasaki/UTK-4/09 (H1N1)					
	Day 3 after infection			Day 7 after infection			Day 3 after infection			Day 7 after infection		
	1	2	3	4	5	6	7	8	9	10	11	12
Nasal mucosa	4.7	3.3	–	–	–	–	–	–	–	–	–	–
Oro/nasopharynx	6.3	4.4	4.7	–	7.9	–	–	–	4.3	–	–	4.8
Tonsil	6.4	–	–	–	7.1	–	–	–	2.8	–	–	3.0
Trachea	5.9	2.0	5.6	–	–	–	2.0	4.1	–	3.7	–	5.4
Bronchus (right)	5.7	2.9	4.3	–	5.1	–	–	2.5	–	3.5	–	3.8
Bronchus (left)	5.9	–	6.1	–	5.1	–	–	–	–	3.3	–	5.1
Lung (upper right)	5.7	5.6	4.5	–	–	–	2.7	–	–	–	–	–
Lung (middle right)	5.6	6.4	6.9	–	–	–	2.3	2.6	2.5	–	–	–
Lung (lower right)	6.1	4.5	6.0	–	–	–	2.6	2.6	–	–	–	3.4
Lung (upper left)	4.7	4.3	6.4	–	–	–	–	–	–	–	–	–
Lung (middle left)	5.8	4.3	6.3	–	–	–	–	–	–	–	–	–
Lung (lower left)	6.7	4.5	6.6	–	–	–	–	–	–	–	–	2.3
Conjunctiva	3.6	–	–	–	–	–	–	–	–	–	–	–

Cynomolgus macaques were inoculated with $10^{7.4}$ p.f.u. of virus (6.7 ml) through multiple routes (see Methods). Three macaques per group were killed on days 3 and 7 after infection for virus titration. No virus was recovered from lymph nodes (chest), heart, spleen, kidneys or liver of any of the animals. A dash indicates that virus was not detected (detection limit: 2 $\log_{10}$ p.f.u. g^{-1}). Numbers 1 to 12 indicate animal identification number. Values indicate virus titre (mean $\log_{10}$ p.f.u. g^{-1}).

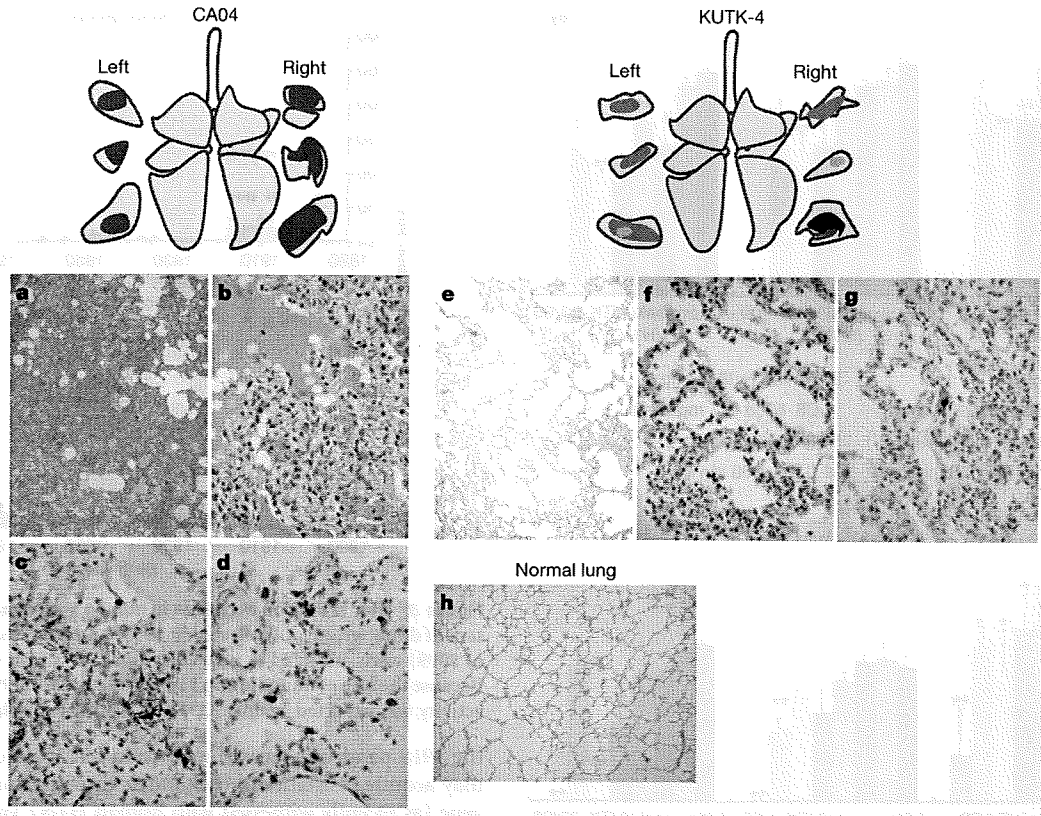

Figure 1 | Pathological examination of the lungs of infected cynomolgus macaques. **a–h**, Representative pathological images of CA04-infected (macaque no. 1, **a–d**), KUTK-4-infected (macaque no. 7, **e–g**) and mock-infected (**h**) lungs on day 3 after infection. One or two sections per lung lobe were examined. Representative findings are shown to depict the distribution of lesions in the sections (shown as cross-sections placed next to illustrations of each lung lobe), with or without viral antigen, as follows: brown, severe lung lesion containing moderate to many viral-antigen-positive cells; pink, mild lung lesions containing a few viral-antigen-positive cells; blue, lung lesions with alveolar wall thickening, with remaining air spaces unaffected. Original magnification: **a**, **e**, **h**, ×40; **b–d**, **f**, **g**, ×400.

KUTK-4 (Supplementary Fig. 10f and g). Thus, in all three mammalian models tested, CA04 seemed to be more pathogenic than a contemporary human H1N1 virus, KUTK-4.

Efficient human-to-human transmission is a critical feature of pandemic influenza viruses. To assess the transmissibility of CA04, naive ferrets in perforated cages were placed next to ferrets inoculated with 10^6 p.f.u. of CA04 (see Methods for detailed procedures). This experimental setting allows for aerosol transmission (that is, the exchange of respiratory droplets between the inoculated and non-inoculated ferrets) but prevents transmission by direct and indirect contact. All three contact ferrets were positive for CA04 virus on days 3 and 5 after infection (Supplementary Table 4). This transmission pattern is comparable to those of two human control influenza viruses that are known to transmit among ferrets: KUTK-4 and A/Victoria/3/75 (H3N2)[9]. By contrast, an avian influenza virus (A/duck/Alberta/35/76; H1N1) did not transmit (Supplementary Table 4).

Genetic analysis suggests that S-OIV originated in pigs[1]. However, there were no confirmed influenza virus outbreaks in Central American pigs before the reported S-OIV infections in humans. To assess S-OIV replication in pigs, we inoculated specific-pathogen-free miniature pigs, which are easier to manage, with CA04 or a classical swine influenza virus (A/swine/Hokkaido/2/81, H1N1). No signs of disease were observed (data not shown), although both viruses replicated efficiently in the respiratory organs of these animals (Supplementary Tables 5 and 6). Slightly higher titres of CA04 were detected in lungs on day 3 after infection, which is supported by pathological findings that show more apparent bronchitis and bronchiolitis in pigs infected with CA04 (Supplementary Fig. 11). The asymptomatic infection of CA04, despite efficient virus replication, might explain the lack of reports of S-OIV outbreaks in pigs before virus transmission to humans.

Antiviral compounds are the first line of defence against pandemic influenza viruses. Sequence analysis suggests that S-OIVs are resistant to ion channel inhibitors such as amantadine and rimantadine[1]. We therefore tested the licensed neuraminidase inhibitors oseltamivir and zanamivir, the experimental neuraminidase inhibitor R-125489 (the active form of CS-8958[10]) and the experimental compound T-705 (a broad-spectrum viral RNA polymerase inhibitor[11]) for their efficacy against CA04. In cell culture, CA04 was highly susceptible to all compounds tested (Supplementary Table 7), as were the human H1N1 control viruses A/Kawasaki/UTK-23/08 and KUTK-4, with the exception of the known oseltamivir resistance of KUTK-4. Comparable sensitivities were also found in an enzymatic neuraminidase inhibition assay[12] (Supplementary Table 8) and in mice (Fig. 2), consistent with observations in clinical settings.

A recent report suggested that 33% of individuals over 60 years of age had neutralizing antibodies to CA04 (http://www.cdc.gov/mmwr/preview/mmwrhtml/mm5819a1.htm; Morbidity and Mortality Weekly Report, Centers for Disease Control and Prevention), probably due to previous exposure to antigenically similar H1N1 viruses. In fact, both the human H1N1 viruses that circulated until 1957 and the classical swine virus HA gene of S-OIVs are descendants of the 1918 pandemic virus, possibly explaining their antigenic relatedness. In 1977, H1N1 viruses re-emerged that were genetically and antigenically very closely related to viruses circulating in the 1950s[13] and should thus have elicited neutralizing antibodies to CA04 among younger age groups; however, this does not seem to be the case, according to the above described report. To resolve this puzzling finding, we assessed the neutralizing activities of sera collected from a broad range of age groups against CA04 and KUTK-4. We used two sets of donor sera, collected in 1999 from residents and workers in a nursing home (donor set 1), and in April

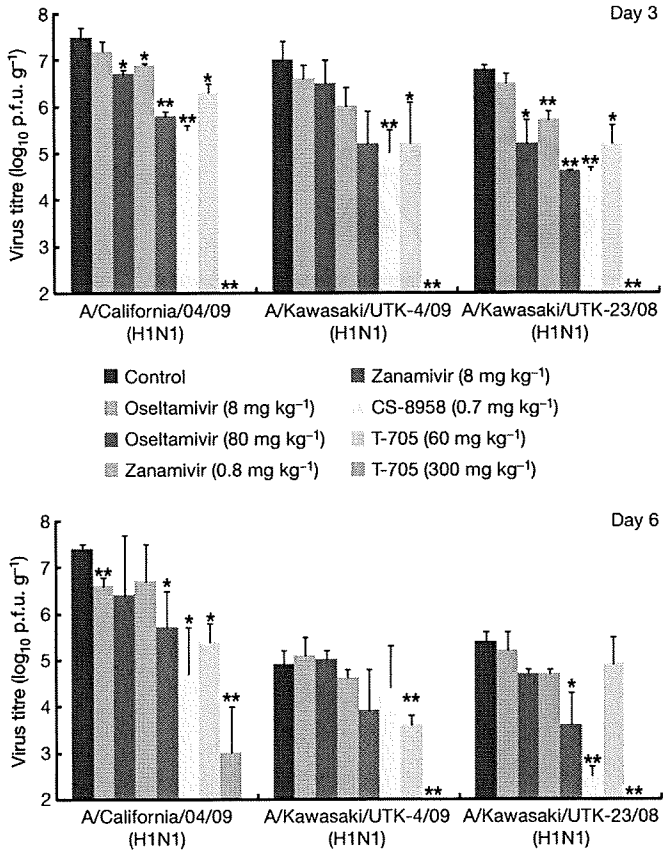

Figure 2 | CA04 sensitivity to antiviral compounds in mice. Mice were intranasally inoculated with 10^4 p.f.u. (50 µl) of CA04, KUTK-4 or A/Kawasaki/UTK-23/08 (H1N1). At 1 h after infection, mice were administered oseltamivir phosphate, zanamivir, CS-8958, T-705, or distilled water and PBS (control). Three mice per group were killed on days 3 and 6 after infection and the virus titres in lungs were determined by plaque assays in MDCK cells; results are reported as means ± s.d. The statistical significance of differences in lung virus titres of control mice and those treated with antivirals were assessed by use of the Student's *t*-test (asterisk, $P < 0.05$; double asterisk, $P < 0.01$).

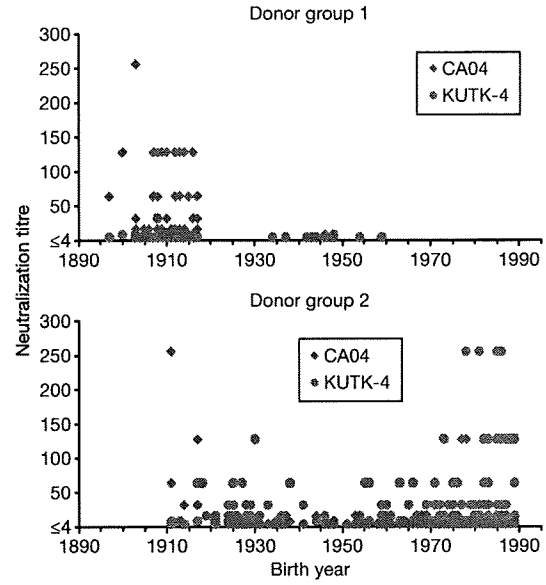

Figure 3 | Neutralization activities in human sera against viruses. Human sera of donor groups 1 (collected in 1999) and 2 (collected in April and May of 2009) were subjected to neutralization assays with CA04 and KUTK-4. Because the sera of donor group 1 were collected in 1999, little neutralization activity was expected against KUTK-4, which was isolated in 2009.

2009 from workers and patients in a hospital (donor set 2). High neutralizing activity against KUTK-4 was detected for many sera in donor set 2 (Fig. 3), but not for sera in donor set 1, probably because these sera were collected before the emergence of the current human H1N1 viruses. Interestingly, with few exceptions, no appreciable neutralizing antibodies against CA04 were found for individuals born after 1920; however, many of those born before 1918 had high neutralizing antibody titres (individual neutralizing antibody titres are shown in Supplementary Table 9). These data indicate that infection with the 1918 pandemic virus or closely related human H1N1 viruses, but not infection with antigenically divergent human H1N1 viruses circulating in the 1920s to 1950s, and again since 1977, elicited neutralizing antibodies to S-OIVs.

Our findings indicate that S-OIVs are more pathogenic in mammalian models than seasonal H1N1 influenza viruses. In fact, the ability of CA04 to replicate in the lungs of mice, ferrets and non-human primates, and to cause appreciable pathology in this organ, is reminiscent of infections with highly pathogenic H5N1 influenza viruses[14], as acknowledged in a recent report by the World Health Organization (http://www.who.int/wer/2009/wer8421/en/index.html). We therefore speculate that the high replicative ability of S-OIVs might contribute to a viral pneumonia characterized by diffuse alveolar damage that contributes to hospitalizations and fatal cases where no other underlying health issues exist (http://www.who.int/wer/2009/wer8421/en/index.html). In addition, sustained person-to-person transmission might result in the emergence of more pathogenic variants, as observed with the 1918 pandemic virus (reviewed in ref. 15). Furthermore, S-OIVs may acquire resistance to oseltamivir through mutations in their NA gene (as recently witnessed with human H1N1 viruses[16]), or through reassortment with co-circulating, oseltamivir-resistant seasonal human H1N1 viruses. Collectively, our findings are a reminder that S-OIVs have not yet garnered a place in history, but may still do so, as the pandemic caused by these viruses has the potential to produce a significant impact on human health and the global economy.

METHODS SUMMARY

Viruses and cells. All swine-origin H1N1 viruses were isolated and passaged in MDCK cells to produce viral stocks. The viruses and their passage histories are described in Methods. All experiments with S-OIVs were performed in approved enhanced biosafety level 3 (BSL3) containment laboratories.

MDCK cells and MDCK cells overexpressing the β-galactoside α2,6-sialyltransferase I gene[17] were maintained in Eagle's minimal essential medium (MEM) containing 5% newborn calf serum. Human airway epithelial (HAE) cells were obtained from residual surgical tissue trimmed from lungs during the process of transplantation. The bronchial specimens were dissected and enzymatically digested, and monolayers of HAE cells were isolated, cultured and differentiated as previously described[18].

Animals. Five- and six-week-old female BALB/c mice (Jackson Laboratory and Japan SLC Inc.), approximately three-to-four-year-old cynomolgus macaques (Ina Research Inc.), five-to-eight-month-old male ferrets (Marshall Farms and Triple F Farms) and two-month-old female specific-pathogen-free miniature pigs (Nippon Institute for Biological Science) were used according to approved protocols for the care and use of animals. Detailed procedures are provided in Methods.

Antiviral sensitivity of viruses in mice. Five-week-old female BALB/c mice (Japan SLC Inc.; groups of six) were anaesthetized with sevoflurane and intranasally inoculated with 10^4 p.f.u. (volume, 50 µl) of CA04, KUTK-4, or A/Kawasaki/UTK-23/08 (H1N1). At 1 h after infection, mice were administered antiviral compounds as described in detail in Methods. Three mice per group were killed on days 3 or 6 after infection and the virus titres in lungs were determined by plaque assays in MDCK cells.

Full Methods and any associated references are available in the online version of the paper at www.nature.com/nature.

Received 2 June; accepted 3 July 2009.
Published online 13 July 2009.

1. Novel Swine-Origin Influenza A (H1N1) Virus Investigation Team. Emergence of a novel swine-origin influenza A (H1N1) virus in humans. *N. Engl. J. Med.* 360, 2605–2615 (2009).

2. Kawaoka, Y. & Webster, R. G. Sequence requirements for cleavage activation of influenza virus hemagglutinin expressed in mammalian cells. *Proc. Natl Acad. Sci. USA* **85**, 324–328 (1988).
3. Hatta, M., Gao, P., Halfmann, P. & Kawaoka, Y. Molecular basis for high virulence of Hong Kong H5N1 influenza A viruses. *Science* **293**, 1840–1842 (2001).
4. Iwakura, Y., Nakae, S., Saijo, S. & Ishigame, H. The roles of IL-17A in inflammatory immune responses and host defense against pathogens. *Immunol. Rev.* **226**, 57–79 (2008).
5. Hamada, H. *et al.* Tc17, a unique subset of CD8 T cells that can protect against lethal influenza challenge. *J. Immunol.* **182**, 3469–3481 (2009).
6. Baskin, C. R. *et al.* Early and sustained innate immune response defines pathology and death in nonhuman primates infected by highly pathogenic influenza virus. *Proc. Natl Acad. Sci. USA* **106**, 3455–3460 (2009).
7. Rimmelzwaan, G. F. *et al.* Pathogenesis of influenza A (H5N1) virus infection in a primate model. *J. Virol.* **75**, 6687–6691 (2001).
8. Kobasa, D. *et al.* Aberrant innate immune response in lethal infection of macaques with the 1918 influenza virus. *Nature* **445**, 319–323 (2007).
9. Maines, T. R. *et al.* Lack of transmission of H5N1 avian-human reassortant influenza viruses in a ferret model. *Proc. Natl Acad. Sci. USA* **103**, 12121–12126 (2006).
10. Yamashita, M. *et al.* CS-8958, a prodrug of the new neuraminidase inhibitor R-125489, shows long-acting anti-influenza virus activity. *Antimicrob. Agents Chemother.* **53**, 186–192 (2009).
11. Furuta, Y. *et al. In vitro* and *in vivo* activities of anti-influenza virus compound T-705. *Antimicrob. Agents Chemother.* **46**, 977–981 (2002).
12. Hayden, F. G. *et al.* Inhaled zanamivir for the prevention of influenza in families. Zanamivir Family Study Group. *N. Engl. J. Med.* **343**, 1282–1289 (2000).
13. Nakajima, K., Desselberger, U. & Palese, P. Recent human influenza A (H1N1) viruses are closely related genetically to strains isolated in 1950. *Nature* **274**, 334–339 (1978).
14. Peiris, J. S. *et al.* Re-emergence of fatal human influenza A subtype H5N1 disease. *Lancet* **363**, 617–619 (2004).
15. Wright, P. F., Neumann, G. & Kawaoka, Y. *Fields Virology* (eds Knipe, D. M. *et al.*) 1691–1740 (Wolters Kluwer/Lippincott Williams & Wilkins, 2007).
16. Moscona, A. Global transmission of oseltamivir-resistant influenza. *N. Engl. J. Med.* **360**, 953–956 (2009).
17. Hatakeyama, S. *et al.* Enhanced expression of an α2,6-linked sialic acid on MDCK cells improves isolation of human influenza viruses and evaluation of their sensitivity to a neuraminidase inhibitor. *J. Clin. Microbiol.* **43**, 4139–4146 (2005).
18. Jakiela, B., Brockman-Schneider, R., Amineva, S., Lee, W. M. & Gern, J. E. Basal cells of differentiated bronchial epithelium are more susceptible to rhinovirus infection. *Am. J. Respir. Cell Mol. Biol.* **38**, 517–523 (2008).

Supplementary Information is linked to the online version of the paper at www.nature.com/nature.

Acknowledgements We thank the Centers for Disease Control (CDC) for A/California/04/09 virus and R. Fouchier for A/Netherlands/603/09 virus. We thank K. Wells for editing the manuscript, and M. McGregor, R. Moritz, A. Hanson, H. Ishida, H. Tsuchiya, R. Torii, N. Yamamoto, K. Soda, N. Nomura and H. Yoshida for technical assistance. We also thank T. Umemura, Y. Sunden and T. Tanaka for pathological analyses of virus-infected pigs. This work was supported by National Institute of Allergy and Infectious Diseases Public Health Service research grants, by an NIAID-funded Center for Research on Influenza Pathogenesis (CRIP, HHSN266200700010C), by Grant-in-Aid for Specially Promoted Research, by a contract research fund for the Program of Founding Research Centers for Emerging and Reemerging Infectious Diseases from the Ministry of Education, Culture, Sports, Science and Technology, and by grants-in-aid from the Ministry of Health and by ERATO (Japan Science and Technology Agency).

Author Contributions Y.I., K.S., M.K., T.W., Y.S., M.H., Y.M., D.T., Y.S.-T., T.N., M. Imai, S.W., K.I.-H., T.H., N.S., H.K., K.O. and Y.K. designed the experiments; Y.I., K.S., M.K., T.W., Y.S., M.H., D.T., Y.S.-T., T.N., S.S., M. Imai, Y.H., S.W., C.L., S.Y., K.F., S.M., H. Imai, S.K., M. Ito, R.T., K.I.-H., M.S., T.H., Kei Takahashi, A.M., H. Ishigaki, M. Nakayama, M. Okamatsu, Kazuo Takahashi, D.W., P.A.S., R.S., H.S., Y.F., M. Yamashita, K.M., K.N., M. Nakamura, R.B.-S., J.G., H.M. and M. Yamazaki performed the experiments; Y.I., K.S., M.K., T.W., Y.S., M.H., Y.M., Y.S.-T., T.N., M. Imai, S.W., C.L., S.Y., K.I.-H., T.H., H.G., M.S., M. Ozawa, G.N., H.K., K.O. and Y.K. analysed data; Y.I., K.S., M.K., T.W., Y.S., M.H., Y.M., Y.S.-T., T.N., M. Imai, K.I.-H., M.S., M. Ozawa, G.N., K.O. and Y.K. wrote the manuscript. Y.I., K.S., M.K., T.W., Y.S., M.H. and Y.M. contributed equally to this work.

Author Information Reprints and permissions information is available at www.nature.com/reprints. The authors declare competing financial interests: details accompany the full-text HTML version of the paper at www.nature.com/nature. Correspondence and requests for materials should be addressed to Y.K. (kawaokay@svm.vetmed.wisc.edu).

METHODS

Viruses. A/California/04/09 (H1N1; CA04) was provided by the Centers for Disease Control (CDC). A/Wisconsin/WSLH049/09 (H1N1) was isolated from a patient with mild symptoms, whereas A/Wisconsin/WSLH34939/09 (H1N1) was isolated from a hospitalized patient. A/Netherlands/603/09 (H1N1) was isolated from a patient with mild symptoms and was provided by R. Fouchier. A/Osaka/164/09 (H1N1) was also isolated from a patient with mild symptoms.

The following influenza viruses served as controls: A/Kawasaki/UTK-4/09 (H1N1; KUTK-4; passaged twice in MDCK cells), an oseltamivir-resistant seasonal human virus; A/WSN/33 (H1N1; generated by reverse genetics and passaged twice in MDCK cells), a typical spherical influenza virus[19]; A/Kawasaki/UTK-23/08 (H1N1; passaged twice in MDCK cells), an oseltamivir-sensitive seasonal human virus; A/Victoria/3/75 (H3N2; passaged several times in eggs after it was obtained from the CDC), a human virus; A/swine/Hokkaido/2/81 (H1N1; passaged several times in eggs), a classical swine virus; and A/duck/Alberta/35/76 (H1N1; passaged several times in eggs), an avian virus. All experiments with S-OIV viruses were performed in enhanced biosafety level 3 (BSL3) containment laboratories at the University of Wisconsin-Madison, which are approved for such use by the CDC and the US Department of Agriculture, or in BSL3 containment laboratories at the University of Tokyo, the Shiga University of Medical Science, or the Hokkaido University, all of which are approved for such use by the Ministry of Agriculture, Forestry and Fisheries, Japan.

Viral pathogenesis in mice. Six-week-old female BALB/c mice (Jackson Laboratory and Japan SLS Inc.) were used in this study. Baseline body weights were measured before infection. Three mice per group were anaesthetized with isoflurane and intranasally inoculated with 10^2, 10^3, 10^4, or 10^5 p.f.u. (50 μl) of CA04 and KUTK-4, or undiluted virus from virus stocks (CA04, $10^{6.5}$ p.f.u.; KUTK-4, $10^{6.6}$ p.f.u.). Body weight and survival were monitored daily for 14 days and mice with body weight loss of more than 25% of pre-infection values were killed. For virological and pathological examinations, 6 mice per group were intranasally infected with 10^5 p.f.u. of S-OIVs and KUTK-4 and 3 mice per group were killed on days 3 and 6 after infection. The virus titres in various organs were determined by plaque assays in MDCK cells.

Growth kinetics of virus in human airway epithelial (HAE) cells. Cultures of differentiated HAE cells were washed extensively with PBS to remove accumulated mucus and infected with virus at a multiplicity of infection (MOI) of 0.001 from the apical surface. The inoculum was removed after 1 h of incubation at 35 °C, and cells were further incubated at 35 °C. Samples were collected at 12, 24, 48, 72 and 96 h after infection from the apical surface. Apical harvesting was performed by adding 500 μl of medium to the apical surface, followed by incubation for 30 min at 35 °C, and removal of the medium from the apical surface. The titres of viruses released into the cell culture supernatant were determined by plaque assay in MDCK cells.

Experimental infection of cynomolgus macaques. Approximately three-to-four-year-old cynomolgus macaques (*Macaca fascicularis*) from the Philippines (obtained from Ina Research Inc.), weighing 2.1–3.0 kg and serologically negative by AniGen AIV antibody ELISA, which detects all influenza A virus subtypes (Animal Genetics Inc.), were used in this study. Baseline body weights were established by two or three measurements before infection. Under anaesthesia, telemetry probes (TA10CTA-D70, Data Sciences International) were implanted in the peritoneal cavities of animals to monitor body temperature. Six macaques per group were intramuscularly anaesthetized with ketamine (5 mg per kg) and xylazine (1 mg per kg) and inoculated with a suspension containing $10^{6.5}$ p.f.u. ml^{-1} of CA04 or KUTK-4 virus through a combination of intratracheal (4.5 ml), intranasal (0.5 ml per nostril), ocular (0.1 ml per eye) and oral (1 ml) routes (resulting in a total infectious dose of $10^{7.4}$ p.f.u.). Macaques were monitored every 15 min for changes in body temperature. On days 1, 3, 5 and 7 after infection, nasal and tracheal swabs and bronchial brush samples were collected. On days 3 and 7 after infection, 3 macaques per group were killed for virological and pathological examinations. The virus titres in various organs and swabs were determined by plaque assays in MDCK cells. Experiments were carried out in accordance with the Guidelines for the Husbandry and Management of Laboratory Animals of the Research Center for Animal Life Science at Shiga University of Medical Science, Shiga, Japan, and approved by the Shiga University of Medical Science Animal Experiment Committee and Biosafety Committee.

Experimental infection of ferrets. We used five-to-eight-month-old male ferrets (Marshall Farms and Triple F Farms), which were serologically negative by haemagglutination inhibition (HI) assay for currently circulating human influenza viruses. Baseline body temperatures and body weights were established by one or two measurements before infection. Six ferrets per group were intramuscularly anaesthetized with ketamine and xylazine (5 mg and 0.5 mg per kg of body weight, respectively) and intranasally inoculated with 10^6 p.f.u. (500 μl) of S-OIVs or KUTK-4. On days 3 and 6 after infection, 3 ferrets per group were killed for virological and pathological examinations. The virus titres in various organs were determined by plaque assays in MDCK cells.

Experimental infection of miniature pigs. Two-month-old female specific-pathogen-free miniature pigs (Nippon Institute for Biological Science), which were serologically negative by AniGen AIV antibody ELISA for currently circulating influenza viruses, were used in this study. Baseline body temperatures were measured once before infection. Four pigs per group were intranasally inoculated with $10^{6.2}$ p.f.u. (1 ml) of viruses. Nasal swabs were collected daily. On day 3 after infection, two pigs per group were killed and their tissues collected for examination. On day 14 after infection, the remaining two pigs per group were killed for virological and pathological examinations. Virus titres in various organs and swabs were determined by plaque assays in MDCK cells. The miniature pigs used in this study were housed in self-contained isolator units (Tokiwa Kagaku) at a BSL3 facility and experiments were conducted in accordance with guidelines established by the Animal Experiment Committee of the Graduate School of Veterinary Medicine, Hokkaido University, Japan.

Pathological examination. Excised tissues of the nasal turbinates, trachea and/or lungs of killed mice, macaques, ferrets and pigs were preserved in 10% phosphate-buffered formalin. Tissues were then processed for paraffin embedding and cut into 5-μm-thick sections. One section from each tissue sample was stained using a standard haematoxylin-and-eosin procedure, whereas another one was processed for immunohistological staining with an anti-influenza virus rabbit antibody (R309; prepared in our laboratory) that reacts comparably with CA04 and KUTK-4. Specific antigen–antibody reactions were visualized by 3,3′-diaminobenzidine tetrahydrochloride staining using a Dako EnVision system (Dako Co. Ltd).

Ferret transmission study. For transmission studies in ferrets, animals were housed in adjacent transmission cages that prevent direct and indirect contact between animals but allow spread of influenza virus through the air. Three or two 5-to-8-month-old ferrets were intranasally inoculated with 10^6 p.f.u. (500 μl) of CA04, KUTK-4, A/Victoria/3/75 (H3N2) or A/duck/Alberta/35/76 (H1N1) (inoculated ferrets). One day after infection, three or two naive ferrets were each placed in a cage adjacent to an inoculated ferret (contact ferrets). All ferrets were monitored daily for changes in body temperature and weight, and the presence of clinical signs. To assess viral replication in the upper respiratory tract, viral titres were determined in nasal washes collected from virus-inoculated and contact ferrets on day 1 after inoculation or co-housing, respectively, and then every other day (up to 9 days).

Cytokine and chemokine measurement. For cytokine and chemokine measurement, homogenates of mouse lungs were processed with the Bio-Plex Mouse Cytokine 23-Plex and 9-Plex panels (Bio-Rad Laboratories), whereas macaque lung homogenates were measured with the MILLIPLEX MAP Non-human Primate Cytokine/Chemokine Panel–Premixed 23-Plex (Millipore). Array analysis was performed by Bio-Plex Protein Array system (Bio-Rad Laboratories).

Antiviral sensitivity of viruses in mice. To test the antiviral sensitivity of viruses in mice, animals were infected as described in the Methods Summary section and 1 h later administered the following antiviral compounds: (1) oseltamivir phosphate: 8 or 80 mg per kg per 400 μl (divided into two oral administrations per day) for 5 days; (2) zanamivir: 0.8 or 8 mg per kg per 50 μl in one daily intranasal administration for 5 days; (3) CS-8958: 0.7 mg per kg per 50 μl in one intranasal administration; (4) T-705: 60 or 300 mg per kg per 400 μl (divided into two oral administrations per day) for 5 days; (5) or distilled water orally (200 μl) and PBS intranasally (50 μl). Three mice per group were killed on day 3 or 6 after infection and the virus titres in lungs were determined by plaque assays in MDCK cells.

Sensitivity to antiviral compounds in tissue culture. MDCK cells overexpressing the β-galactoside α2,6-sialyltransferase I gene (or, for studies with T-705, regular MDCK cells) were infected with CA04, KUTK-4, or A/Kawasaki/UTK-23/08 (H1N1) at a multiplicity of infection of 0.001. After incubation for 1 h at 37 °C, growth medium containing various concentrations of oseltamivir carboxylate (the active form of oseltamivir), zanamivir, R-125489 (the active form of CS-8958), or T-705 was added to the cells. Twenty-four hours later, the culture supernatants were harvested and the 50% tissue-culture infectious dose ($TCID_{50}$) in MDCK cells determined. On the basis of the $TCID_{50}$ value, the 90% inhibitory concentration (IC_{90}) was calculated.

Neuraminidase inhibition assay. To assess the sensitivity of viruses to neuraminidase inhibitors (that is, oseltamivir, zanamivir and CS-8958), neuraminidase inhibition assays were performed as described previously[20]. Briefly, diluted viruses were mixed with various concentrations of oseltamivir carboxylate, zanamivir, or R-125489 in 2-(*N*-morpholino)ethanesulphonic acid containing calcium chloride, and incubated for 30 min at 37 °C. Then, we added methylumbelliferyl-*N*-acetylneuraminic acid (Sigma) as a fluorescent substrate to this mixture. After incubation for 1 h at 37 °C, sodium hydroxide in 80% ethanol was added to the mixture to stop the reaction. The fluorescence of the solution was measured at an